THE ASTROPHYSICAL JOURNAL, 261:115–134, 1982 October 1

ON THE NATURE OF BIPOLAR SOURCES IN DENSE MOLECULAR CLOUDS

ARIEH KÖNIGL
Astronomy Department, University of California, Berkeley
Received 1982 February 1; accepted 1982 April 9

ABSTRACT

A unified interpretation is presented of bipolar sources associated with young stellar objects which are embedded in dense molecular clouds. It is suggested that such phenomena as optical and radio "jets," high-proper-motion Herbig-Haro objects, separating broad-wing CO emission-line lobes, and cometary and bipolar nebulae, are linked through a basic outflow mechanism which is manifested on different scales. The outflow is assumed to originate in a spherically symmetric stellar wind which expands in a medium with anisotropic density and pressure distributions. The wind creates an interstellar bubble which elongates in the direction of the steepest external density gradient. The shape of the evacuated cavity is calculated explicitly for an energy-driven bubble and a power-law density distribution. It is shown that for density distributions which are likely to exist in protostellar environments, the expanding bubble could become unstable to the formation of de Laval nozzles which channel the flow into two oppositely directed, supersonic jets. The structure of nozzles and of jets is discussed in relation to various morphological features of bipolar sources. In particular, certain wave phenomena in jets, which could be induced by variations in the external pressure distribution, are applied to the interpretation of fan-shaped cometary nebulae and of certain stationary Herbig-Haro objects. Herbig-Haro objects with large directed proper motions are interpreted as dense clumps of matter which are accelerated by well-collimated, supersonic jets. Separating CO emission-line lobes are identified with layers of shocked cloud material which are swept up by two oppositely directed jets or by an elongating bubble. Bipolar nebulae are similarly interpreted in terms of an outflow into an anisotropic medium, and it is suggested that certain cometary nebulae could have formed after a bubble or jets broke out on one side of a dense cloud but not on the other. It is argued, on the basis of the near-alignment which is found in some sources between the bipolar axis and the measured polarization vectors, that the magnetic field in the cloud could have determined the orientation of at least some of the bipolar sources. (The other plausible mechanism for producing a large-scale anisotropy in the cloud is rotation.) It is suggested that the ambient magnetic field could influence the expansion of an interstellar bubble both directly, by the action of magnetic stresses on the boundary, and indirectly, through its effect on the external density distribution. In addition, it is shown that the presence of an ordered magnetic field and of a strong central UV source could lead to an apparent bipolar CO emission pattern even when the bubble remains spherical. Finally, theoretical advantages of a directed-outflow model for bipolar sources are considered, and the relevance of molecular cloud jets to the study of jets in other astrophysical environments is briefly outlined.

Subject headings: hydrodynamics — interstellar: magnetic fields — interstellar: molecules — nebulae: general — stars: mass loss — stars: pre–main-sequence — stars: winds

I. INTRODUCTION

It has been known for some time now that relatively large velocity fields exist in regions of active star formation within dense molecular clouds. However, only recently has it become apparent that, in some cases at least, these motions are not chaotic, but in fact represent a systematic outflow from a heavily obscured young star or protostar (e.g., Downes *et al.* 1981; Genzel *et al.* 1981). Moreover, there is growing evidence that in many of these sources the outflow, at least on the larger scales ($\sim 10^{18}$ cm), is bipolar in nature, and that in some cases it may even be highly collimated (e.g., Cohen 1982). A representative source of this kind is IRS 5 in the molecular cloud L1551. CO emission-line observations (Snell, Loren, and Plambeck 1980) revealed two lobes, located symmetrically on opposite sides of the embedded infrared source at projected distances of ~ 0.5 pc, and moving away from IRS 5 with radial velocities ~ 15 km s^{-1}. Other broad-wing CO emission-line sources were found to have a similar morphology, with two oppositely directed CO lobes separating from an embedded infrared source. At present, they include Cep A (Rodríguez, Ho, and Moran 1980), GL 490 (Lada and Harvey 1981), NGC 1333 (Snell and Edwards

1981), and NGC 2068 (Snell and Edwards 1982), with new sources being continuously added to the list. (R Mon is another source in which CO lobes appear to be separating, albeit with much lower velocities; Cantó *et al.* 1981.) All of these sources have comparable projected distances (0.1–0.5 pc) and separation velocities (15–25 km s^{-1}) from the central star, which suggests that they are members of a single class of objects (Lada and Harvey 1981). However, the inferred mass of the high-velocity gas and the measured infrared luminosity vary significantly from source to source.

The evidence for directed outflow in L1551 comes also from the measured proper motions of two Herbig-Haro objects (HH 28 and HH 29) which are located between IRS 5 and the SW CO lobe (Cudworth and Herbig 1979). These objects move along the CO lobe with velocities approaching 200 km s^{-1}, and their velocity vectors intersect at an angle of $\sim 15°$ near IRS 5. Substantial proper motions along the axis of the CO lobes have been reported also for the nuclei of HH 39, which appear to move away from R Mon (Herbig and Jones 1981). A similar, and even more striking, example of a directed outflow involving Herbig-Haro objects is provided by HH 1 and HH 2 in the Orion complex (Herbig and Jones 1981). These objects are located on opposite sides of what is apparently a dust-shrouded young star, and are each composed of a number of individual knots which move away from the central source with nearly parallel velocities of up to ~ 350 km s^{-1}. In the case of NGC 1333, a string of Herbig-Haro objects (HH 7–11) with blueshifted radial velocities as large as ~ 150 km s^{-1} (Strom, Grasdalen, and Strom 1974) lie within the blueshifted CO lobe, and are aligned with the separation axis of the lobes. This again points to a common origin for the motions of both the CO lobes and the Herbig-Haro objects in a directed outflow from the central young star. That the bipolar pattern of the outflow in L1551 is established already on a scale of $\lesssim 10^{15}$ cm is indicated by a radio continuum map of IRS 5 (Cohen, Bieging, and Schwartz 1982), which reveals a $\sim 10^{16}$ cm feature elongated roughly in the direction of the CO lobes, but unresolved in the transverse direction. The radio feature coincides with an optical "jet" which is visible on a photograph of this region (Strom, Grasdalen, and Strom 1974). These results also indicate that the outflow in this source did not occur in a single event some 10^4 yr ago (the inferred dynamical time scale of the CO lobes), but that, in fact, it is still going on at the present time.

In this paper, the bipolar outflow from young stellar objects embedded in dense molecular clouds is interpreted in terms of a spherically symmetric, supersonic stellar wind which flows into an ambient medium with anisotropic density and pressure distributions. The wind evacuates an interstellar bubble which elongates in the direction of the steepest external density gradient. For certain density distributions which may characterize a protostellar environment, the boundary of the bubble could become unstable to the formation of nozzles that channel the flow into two oppositely directed, supersonic jets. After the jets are formed, they may be confined and collimated by the pressure of the medium through which they propagate. The jets will accelerate any dense clumps of matter that lie in their paths, or that are entrained in the flow; the accelerated clumps could attain the jet velocity, and may be identified with the high-proper-motion Herbig-Haro objects. As long as the bubble or the jets are confined to the molecular cloud, they push ahead of them dense layers of shocked and swept-up ambient material. These layers move at much lower velocities than the material in the jets, and could be identified with the broad-wing molecular emission-line lobes. After the ends of the bubble or the jets emerge through the boundary of the cloud, they could be perceived as a cometary or a bipolar nebula (e.g., Cohen 1974; Calvet and Cohen 1978). This model thus provides a unified interpretation of the various bipolar phenomena that are observed in different spectral regimes and on different length scales in the vicinity of embedded infrared sources. The basic assumption of this model—namely, that the observed bipolar outflow is produced by the interaction of a spherically symmetric stellar wind with an anisotropic confining medium—is the same as in the model of Cantó (1980; see also Cantó and Rodríguez 1980, Barral and Cantó 1981). However, the two models are otherwise quite different, especially in their interpretation of Herbig-Haro objects. The discussion of jets in this paper is patterned after the original "twin beam" model of extragalactic radio sources (Blandford and Rees 1974), according to which the outer lobes are powered by jets which emanate in two opposite directions from the central active galactic nucleus. In fact, we argue that the jet formation and propagation mechanisms described in that model are likely to operate also under the conditions which prevail on the much smaller scale of a protostellar environment. In this scenario, the high-velocity molecular emission lobes are the counterparts of the extended double radio lobes, whereas Herbig-Haro objects could be the analogs of the emission knots often observed in extragalactic jets (cf. Blandford and Königl 1979*a*).

The two key elements of our model are a source of strong stellar wind and a surrounding flattened mass distribution. A direct measurement of wind parameters near the source of bipolar outflow has so far been reported only for GL 490 (Simon *et al.* 1981), where a wind kinetic power of order $L_\odot$ has been estimated. However, similarly strong winds have been inferred to exist in a number of pre-main-sequence stars (e.g., Kuhi 1964; Garrison 1978), and may thus be expected also in the other bipolar sources. The origin of these winds is not yet clearly understood (e.g., DeCampli 1981), but the nature of the driving mechanism is not directly relevant to the discussion in this paper. As regards the other key ingredient of the model, there now exists observational evidence for a flattened mass distribution in a number of young stellar objects. These include IRS 5, where an elongated ($\sim 10^{16}$ cm), dusty "disk," oriented roughly at right angles to the radio and optical "jet," is indicated by 10 μm infrared measurements (Beichman and Harris

1980); and GL 961 (Harvey, Campbell, and Hoffmann 1977), another high-velocity CO emission source, which is also associated with a cometary nebula (Blitz and Thaddeus 1980). The present model differs, however, from some previous models (e.g., Elmegreen 1978; Icke 1981) in which the anisotropy of the outflow arises because of the geometrical properties of a thin disk. The geometry envisioned in this paper is rather that of an oblate cloud which, initially, totally surrounds the central star. After the ends of the bubble or the jets break through the poles, the cloud would appear as a thick disk, or torus, centered on the star. Such structures have in fact been inferred to exist near the apexes of several cometary and bipolar nebulae associated with young stars (e.g., Cantó *et al.* 1981; Cohen *et al.* 1981). The flattening of the gas distribution around the central source could be due to rotation, as proposed in the original "twin beam" model. Alternatively, if the molecular cloud is strongly magnetized, and if it contracts under "flux freezing" conditions, then the direction of the steepest density gradient could coincide with the original direction of the magnetic field (see Mouschovias 1976). This possibility is suggested in L1551 (and in several other molecular clouds containing bipolar sources) by the fact that the axis of the central "jet" and of the CO lobes, as well as the velocity vectors of the Herbig-Haro objects HH 28 and HH 29, lies roughly in the direction of the local magnetic field, as inferred from optical polarization measurements of background stars (Vrba, Strom, and Strom 1976). These measurements also indicate that the magnetic field in these clouds, and particularly in L1551, remains fairly well ordered on the scale of the aligned CO lobes.

The plan of this paper is as follows: the evolution of an interstellar bubble in an anisotropic medium is considered in § II. The formation and propagation of jets, and their relation to the various bipolar phenomena observed in molecular clouds, are discussed in § III. The possible role of magnetic fields in producing bipolar emission sources is examined in § IV. Section V contains a summary of the principal results.

II. EXPANSION OF AN INTERSTELLAR BUBBLE IN AN ANISOTROPIC MEDIUM

In this section we consider the evolution of an interstellar bubble which is created by the interaction of a strong stellar wind with a dense ambient medium. We first calculate the spherically symmetric expansion in a medium with isotropic but inhomogeneous density distribution, and then estimate the departure from sphericity in the presence of an anisotropic medium. Our purpose is to illustrate how the degree of elongation of the bubble at the various phases of its evolution depends on the external density distribution. In addition, these results are applied in the next section to the question of jet formation.

Consider a wind blown out with constant kinetic power L_w and velocity V_w from a young stellar object located inside a dense molecular cloud. The expanding wind drives a shock wave into the ambient medium which sweeps up the surrounding material into a thin circumstellar shell and creates an "interstellar bubble" (e.g., Pikel'ner 1968). For the high densities which are typical of protostellar environments, this shock is strongly radiative and gives rise to a highly compressed, cold shell. The wind itself is stopped in another shock wave interior to the shell. If the density of the shocked stellar wind is sufficiently high for the cooling time scale to be shorter than the dynamical time scale of the bubble, then the inner shock will also be radiative, in which case the "snowplowing" shell will be driven essentially by the ram pressure of the wind (e.g., Steigman, Strittmatter, and Williams 1975). For an expansion into an isotropic medium, the momentum and mass conservation equations for the shell are

$$\frac{d}{dt}(M_s V_s) = 4\pi R_s^2 p\,, \tag{1}$$

$$\frac{d}{dt} M_s = 4\pi R_s^2 V_s \rho_e\,, \tag{2}$$

where M_s, R_s, V_s are, respectively, the mass, radius, and velocity of the shell; ρ_e is the external density; and p is the driving pressure, which is set equal to $L_w/2\pi R_s^2 V_w$. (It is assumed that the external pressure p_e is negligible in comparison with p.) Using an external density distribution of the form $\rho_e(R) = AR^{-m}$ $(0 \le m < 3)$, the radius of the shell at sufficiently large values of t is found to be

$$R_s(t) = \left[\frac{(3-m)(4-m)L_w}{4\pi A V_w}\right]^{1/(4-m)} t^{2/(4-m)}\,. \tag{3}$$

Even if the radiative cooling time of the shocked stellar wind is initially shorter than the travel time of the shell, the inequality may eventually be reversed if V_w and m are sufficiently large, at which stage the interior of the bubble becomes hot and nearly isobaric. The subsequent evolution is determined by the energy conservation equation

$$\frac{dE}{dt} = L_w - 4\pi R_s^2 p V_s\,, \tag{4}$$

where the internal energy E is given by

$$E = 2\pi R_s^3 p \tag{5}$$

(Castor, McCray, and Weaver 1975; Weaver *et al.* 1977; Shull 1980). Using equations (1), (2), (4), (5) and a power-law external density distribution, one obtains

$$R_s(t) = \left[\frac{(5-m)^3(3-m)L_w}{6\pi(7-2m)(11-m)A}\right]^{1/(5-m)} t^{3/(5-m)}\,. \tag{6}$$

We estimate that, for $m > 1/2$, this solution would be valid beyond the transition radius R_t, obtained by equating the dynamical time scale $t(R_s)$ (from eq. [6]) with the cooling time $t_c = 4.9 \times 10^{-22} T_{sw}^{1.6} \rho_{sw}^{-1}$ (e.g., Hollenbach and McKee 1979), where $T_{sw} = 1.5 \times 10^{-9} V_w^2$ K and

$$\rho_{sw} = \frac{5(5-m)}{2\pi(11-m)} \frac{L_w t}{V_w^2 R_s^3}$$

are, respectively, the temperature and density of the shocked wind. The expressions for T_{sw} and ρ_{sw} are calculated under the assumption that the mass outflow rate in the wind, $\dot{M}_{out} = 2L_w/V_w^2$, is larger than the mass evaporation rate from the shell, $\dot{M}_{ev} = 1.75 \times 10^{-14} T^{5/2} R_s \text{ g s}^{-1}$, which should be valid for $R_s < R_e = 1.4 \times 10^{36} L_w/V_w^7$ cm. These approximations give

$$R_t = \left\{1.56 \times 10^{36} \left[\frac{(7-2m)}{(3-m)(11-m)^{1/2}(5-m)^{3/2}}\right]^{2/3} \times \left(\frac{L_w^{1/3} A^{2/3}}{V_w^{5.2}}\right)\right\}^{3/(2m-1)} \text{cm}. \quad (7)$$

When $R_s > R_e$, the cooling can be estimated using the expressions for the internal temperature and density in Weaver *et al.* (1977). Formally, we find that, for typical parameters, the inequality $t_c > t(R_s)$ will continue to hold throughout the evolution of the bubble if $m > 1.61$. In practice, however, a bubble with $\dot{M}_{ev} > \dot{M}_{out}$ is expected to act as a self-regulating thermostat, and to evolve in a manner which is intermediate between the momentum-driven case, equation (3), and the energy-driven case, equation (6) (see Weaver *et al.* 1977).

If the ambient medium is anisotropic, then the bubble does not remain spherical, but instead elongates in the direction of the steepest external density gradient. In a cloud which is in hydrostatic equilibrium, this direction could coincide with that of the local rotation axis or of the "frozen-in" magnetic field, if either centrifugal forces or magnetic stresses are dynamically important in opposing gravitational contraction. (An ambient magnetic field could thus have an indirect effect on the expansion of the shell through its influence on the density distribution in the cloud; the direct dynamical interaction between the magnetic field and the bubble is discussed in § IV and the Appendix.) If the density distribution possesses cylindrical as well as reflection symmetry, then a cross section of the bubble in a plane containing the axis of symmetry would have the shape of two fans connected at the origin. A similar configuration arises in the case of a stationary bubble supported by an anisotropic pressure distribution (see Cantó 1980). A general formulation for calculating the detailed shape of a bubble in the thin-shell approximation was presented by Giuliani (1982). In the case of an energy-driven bubble in a one-dimensional density distribution, one can obtain the approximate shape of the shell analytically by the method of the Kompaneets (1960) solution to a point explosion in an exponential atmosphere. This method is described in part (*a*) of the Appendix, where it is applied to a power-law density distribution $\rho_e(z) = Az^{-m}$. (A density distribution of this form leads to a self-similar expansion if the source is located at the origin.) When the value of the power-law exponent m is either 1 or 2, it is possible to write down the solution in closed form. The shapes of the bubble in these two cases are given by equations (A4) and (A5), respectively, and are displayed in Figure 1.

In the next section we shall be concerned with the conditions under which the shell is accelerating. In the case of a power-law density distribution (either spherical or one-dimensional), the criterion for acceleration in both an energy-driven and a momentum-driven expansion is that the power-law exponent m of the distribution be greater than 2 (see eqs. [3] and [6], and discussion in the Appendix). However, if the external pressure is dynamically important, then an energy-driven bubble in a one-dimensional density distribution could be accelerated even if m is less than 2, provided that the pressure distribution is also anisotropic. An extreme example of this behavior, involving a magnetic-pressure-dominated region with a uniform magnetic field, is outlined in the Appendix [part (*b*)]. In this example, the ends of the bubble accelerate already for $m > 0$ [eq. [A8]). However, in less extreme cases, when the external pressure distribution is more isotropic, the transition to accelerated motion would occur at larger values of m.

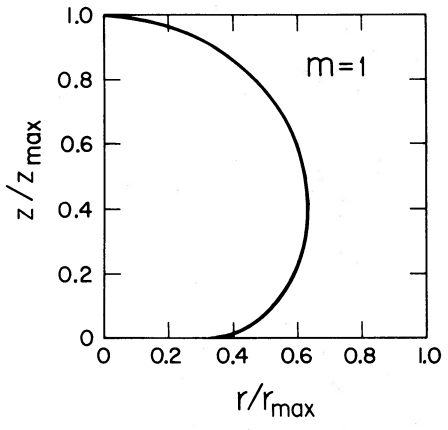

FIG. 1*a*

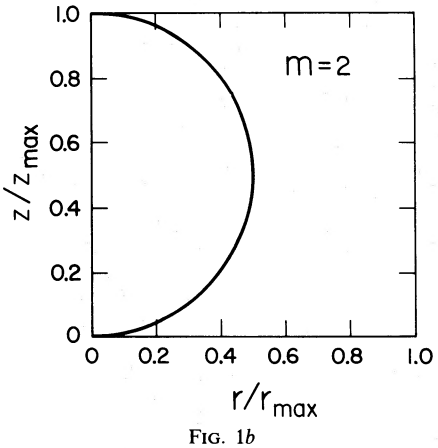

FIG. 1*b*

FIG. 1.—Self-similar shapes of an energy-driven interstellar bubble expanding from the origin in a power-law external density distribution $\rho_e(z) = Az^{-m}$. Figs. 1*a* and 1*b* correspond to the cases $m = 1$ and $m = 2$, respectively, and represent analytic solutions based on the Kompaneets (1960) approximation (eqs. [A4] and [A5] in the Appendix). The bubbles represented in these plots possess cylindrical symmetry about the z-axis, as well as reflection symmetry about the plane $z = 0$.

III. FORMATION AND PROPAGATION OF JETS

a) Establishment of de Laval Nozzles

In this section we examine the possibility that an interstellar bubble elongating in the direction of the steepest external density gradient may evolve into two oppositely directed supersonic jets. Such jets could channel the outflow of a spherically symmetric wind if the wind is first shocked and then passes through two de Laval nozzles (e.g., Courant and Friedrichs 1948), where the flow becomes supersonic again. The jets are most likely to form when the bubble is in the energy-driven snowplow phase, since in this case the internal energy of the shocked stellar wind is not radiated away, and so it is available for reconversion into kinetic energy of directed flow. It is, nevertheless, conceivable that nozzles could also evolve directly from a momentum-driven bubble (see § III*b*). However, in the following discussion we concentrate on the energy-driven phase. One plausible condition for the establishment of nozzles in this case is that the outer ends of the shell (which move with a velocity V_z at a distance z from the center) are accelerated in the direction of elongation. The bubble is then subject to the Rayleigh-Taylor instability (cf. Weaver *et al.* 1977), which would grow on a time scale $\sim[z/(dV_z/dt)]^{1/2}$, and which could lead to the formation of nozzles, as discussed in the next paragraph. (An accelerating shell will be subject to this instability also in the momentum-driven phase.) Another effect which could contribute to the development of nozzles in an accelerating shell is the "breaking away" of the outer ends of the shell from the main body of the bubble, and the concomitant generation of rarefaction waves that travel into the bubble and accelerate the shocked stellar wind in two opposite directions. The detachment of the outer ends should occur after a time $\sim V_w/(dV_z/dt)$, when V_z becomes equal to the speed of sound inside the bubble (which is of order V_w). This effect is analogous to the "breaking through" of a strong blast wave propagating into a stratified atmosphere (e.g., Zel'dovich and Raizer 1967), and to the "champagne effect" as manifested, for example, in the context of embedded H II regions (Bodenheimer, Tenorio-Tagle, and Yorke 1979). In the case of an external density distribution that is a power law in distance from the central source, we found in § II that the condition for acceleration along the axis of symmetry is that the power-law exponent m be greater than 2, although even smaller values of m could lead to acceleration after the external pressure becomes dynamically important. (Recall that the condition for acceleration in the momentum-driven phase is, similarly, $m > 2$.)

It is conceivable that de Laval nozzles may form even when the shell is decelerating, as a result of the buoyancy forces acting on the "light" bubble interior in the gravitational field of the central star. When the buoyancy forces are dominant, the boundary of the cavity is subject to the Rayleigh-Taylor instability, which leads to the formation of a "neck" perpendicular to the elongation axis. For a weak central source the neck may pinch off periodically, resulting in a succession of small bubbles which move out along the symmetry axis, whereas if L_w is too large the neck may choke, leading to an isotropic release of mass. However, for intermediate powers the neck is expected to evolve into the nozzle of a continuous supersonic jet; this is the nozzle formation mechanism proposed in the original "twin beam" model (Blandford and Rees 1974), and subsequently verified in numerical work (Wiita 1978; Norman *et al.* 1981*a*; see also Smith *et al.* 1981). As was noted above, this mechanism is expected to operate even if gravitational buoyancy is unimportant, provided that the shell is accelerating. In order to estimate the range over which the buoyancy forces are dominant, we compare the two main forces which act on the hot gas in the interior of the bubble, viz., the outward-directed buoyancy force and the inward-directed force exerted by the decelerating shell (cf. Gull and Northover 1973). The radius R_b at which these forces balance for a nearly isotropic density distribution $\rho_e = AR^{-m}$ is given, using equation (6), by

$$R_b = \left[\frac{GM_*}{3(2-m)}\right]^{3/(2m-1)} \left[\frac{6\pi(7-2m)(11-m)A}{(3-m)L_w}\right]^{2/(2m-1)}, \tag{8}$$

where M_* is the mass of the central star. If $m > \frac{1}{2}$, as is likely to be the case in a protostellar environment, then buoyancy dominates for $R < R_b$. It can be seen from equation (8) that R_b increases rapidly when m approaches 2; in fact, as we show below, only for m sufficiently close to 2 will R_b be large enough for buoyancy forces to remain effective until after the bubble enters the energy-driven phase and becomes susceptible to the Rayleigh-Taylor instability. We are thus led to the same conclusion as before, namely, that an interstellar bubble expanding in an anisotropic medium is likely to form de Laval nozzles if the power-law exponent of the external density distribution is close to 2.

It is instructive to examine whether, in view of the above considerations, a protostellar environment is a likely site for jet formation. For this purpose we adopt the collapsing isothermal sphere model of Shu (1977), which should provide at least a qualitative description of a protostellar environment when the departure from sphericity is not too large. In this model the cloud is divided into two main regions: an inner free-fall zone in which $\rho_e(R) = [\dot{M}_{\rm in}/(32\pi^2 GM_*)^{1/2}]R^{-3/2}$, where $\dot{M}_{\rm in}$ is the mass accretion rate onto the central star, and a hydrostatic outer envelope in which $\rho_e(R) = (C_{se}^2/2\pi G)R^{-2}$, where C_{se} is the effective isothermal speed of sound in the cloud. The two regions are separated by an expansion wave which propagates outward at the speed C_{se}. Thus, the density distribution can indeed be modeled by a power law in radius with an exponent close to 2. Consequently, any anisotropy in this distribution which is likely to be present (due to rotation or an untangled magnetic field) could have a strong effect on the expansion of an interstellar bubble, and may lead to the establishment of de Laval nozzles. The mass inflow rate which appears in the expression for $\rho_e(R)$ in this model can be estimated by $\dot{M}_{\rm in} \approx C_{se}^3/G$ (Stahler, Shu,

and Taam 1980). We identify the effective speed of sound C_{se} with the internal velocity dispersion deduced from molecular emission-line widths, which is typically a few km s^{-1} (e.g., Burton 1976), about an order of magnitude larger than the thermal speed of sound. For the purpose of numerical estimates we shall use parameters appropriate to the molecular cloud L1551 and the infrared source IRS 5, which was interpreted as a low-mass pre–main-sequence star with total luminosity $L_* \sim 25\ L_\odot$ (Fridlund *et al.* 1980). For L1551, $C_{se} \approx 1$ km s^{-1} (e.g., Snell 1979), which implies $\dot{M}_{in} \approx 2.4 \times 10^{-4}\ (C_{se}/1\ \text{km s}^{-1})^3\ M_\odot\ \text{yr}^{-1}$. With this normalization the density is $\rho_e(R) = 7.3 \times 10^7\ (C_{se}/1\ \text{km s}^{-1})^3\ (M_*/M_\odot)^{-1/2} R^{-3/2}$ g cm^{-3} in the free-fall region, and $\rho_e(R) = 2.4 \times 10^{16}\ (C_{se}/1\ \text{km s}^{-1})^2 R^{-2}$ g cm^{-3} in the outer envelope. If IRS 5 blows out a strong protostellar wind, then the resulting bubble would enter the energy-driven snowplow phase at the transition radius (eq. [7]):

$$R_t \approx 4.7 \times 10^{15} \left(\frac{C_{se}}{1\ \text{km s}^{-1}}\right)^3 \left(\frac{M_*}{M_\odot}\right)^{-1/2} \times \left(\frac{L_w}{L_\odot}\right)^{1/2} \left(\frac{V_w}{10^3\ \text{km s}^{-1}}\right)^{-7.8} \text{cm}$$

for $m = 3/2$, or

$$R_t = 9.5 \times 10^{15} \left(\frac{C_{se}}{1\ \text{km s}^{-1}}\right)^{4/3} \times \left(\frac{L_w}{L_\odot}\right)^{1/3} \left(\frac{V_w}{10^3\ \text{km s}^{-1}}\right)^{-5.2} \text{cm}$$

for $m = 2$; these estimates are appropriate for $R_t < 5.4 \times 10^{13} (L_w/L_\odot)(V_w/10^3\ \text{km s}^{-1})^{-7}$ cm, which represents the condition $\dot{M}_{ev} < \dot{M}_{out}$ in the notation of § II, and would increase for larger values of R_t. Here L_w is scaled by $L_\odot$, which is of order the inferred kinetic power in the expanding CO shell around IRS 5 (Snell, Loren, and Plambeck 1980), and which therefore represents a lower limit on L_w. The strong dependence of R_t on V_w suggests that an interstellar bubble which expands into a nearly isotropic protostellar environment is not likely to go through an energy-driven phase unless $V_w \gtrsim 10^3$ km s^{-1}. (A lower limit of ~ 200 km s^{-1} on V_w can be deduced for this source from the measured proper motions of the Herbig-Haro objects HH 28 and HH 29 [Cudworth and Herbig 1979]. A direct measurement of V_w could in principle be obtained from high-resolution spectra of Bγ lines [cf. Simon *et al.* 1981].) This conclusion could, however, change if the expansion of the bubble is highly anisotropic, since the different dependence of the internal density on the size of the bubble in this case would also change the functional form of R_t. For instance, if the bubble assumes the shape of an elongating cylinder with constant cross section (as in one of the magnetic confinement examples discussed in § IV), then the bubble goes through an initial energy-driven phase for all values of m up to 3/2, as compared with $m < \frac{1}{2}$ in the spherical case (see eq. [7]). The radius R_t should be compared with the "buoyancy radius" R_b (eq. [8]), which in the free-fall zone is given by $R_b = 1.2 \times 10^{13} (C_{se}/1\ \text{km s}^{-1})^3 \times (M_*/M_\odot)(L_w/L_\odot)$ cm. Gravitational buoyancy forces could play a role in the establishment of nozzles only if $R_t/R_b \lesssim 1$; note from equations (7) and (8) that this ratio is independent of the coefficient A in the external density distribution, and that it formally tends to zero as m approaches 2.

b) *Structure of the Nozzles*

We have considered the conditions under which an interstellar bubble is likely to form de Laval nozzles. Such nozzles could develop even if the central cavity has not yet come into pressure equilibrium with the ambient medium and is still expanding. Once pressure equilibrium has been reached, a stationary configuration would be established, as shown schematically in Figure 2. In this picture the stellar wind is decelerated in a strong spherical shock of radius R_w, and the flow is brought

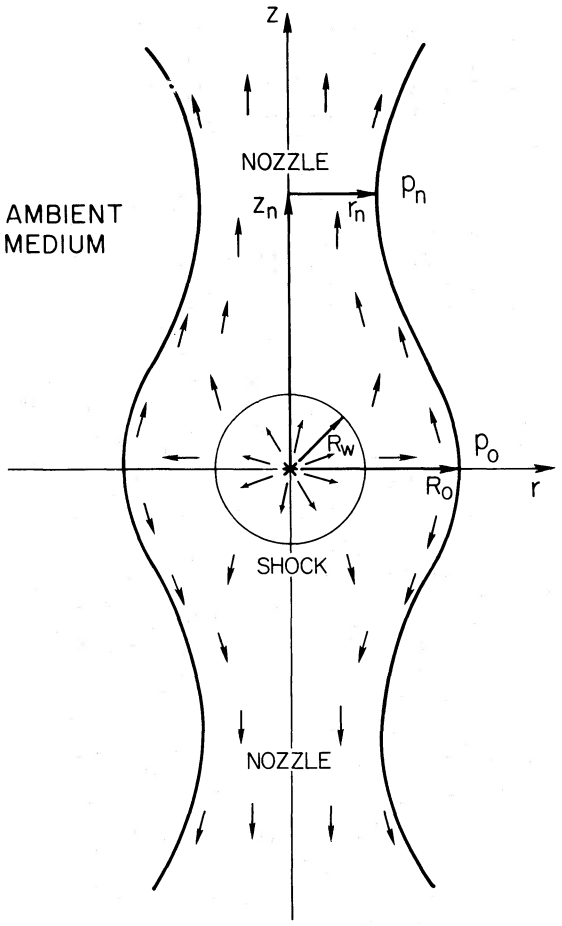

FIG. 2.—Schematic configuration of stationary de Laval nozzles in an axisymmetric external pressure distribution. The pressure drops from the value p_0 in the equatorial plane to p_n at the position of the nozzles. An isotropic, supersonic stellar wind is blown out from the central source and shocked at the radius R_w. It is then reaccelerated in two opposite directions, and becomes supersonic again at $z = z_n$. The arrows indicate the direction of the flow at various locations in the channel.

to a halt in the equatorial plane at the stagnation radius R_0, where the pressure is p_0. (The assumption of a spherical shock is justified if the external pressure distribution is nearly isotropic; see Smith *et al.* 1981.) Along the symmetry axis, however, the shocked wind is reaccelerated, and the flow becomes supersonic again after passing through the de Laval nozzles at a distance z_n from the central source. (Beyond the nozzles the velocity ultimately approaches its initial value V_w.) In order to estimate the parameters of a stable nozzle configuration, we assume that the flow is isotropic throughout with adiabatic index $\Gamma = 5/3$, and that R_0 is sufficiently small that $\dot{M}_{ev}/\dot{M}_{out} \ll 1$ (see § II). If one approximates the flow in the vicinity of the nozzle as one-dimensional, it is then straightforward to show (R. D. Blandford, private communication) that at the nozzle the velocity V_n, the pressure p_n, and the cylindrical radius of the jet r_n satisfy $V_n/V_w = 0.5$, $(p_n/p_0) = (3/4)^{5/2} = 0.49$, and $(r_n/R_w) = (5/4)^{3/4} = 1.18$, respectively. If the jet is in pressure equilibrium with the ambient medium, then the position of the nozzle is determined by the external pressure run. In the one-dimensional approximation, the radius of the jet can be expressed as a function of the external pressure $p_e(z)$, and therefore implicitly as a function of z, by

$$r(z) = \left(\frac{L_w}{5\pi V_w p_0}\right)^{1/2} \left[\frac{p_e(z)}{p_0}\right]^{-3/10} \left\{1 - \left[\frac{p_e(z)}{p_0}\right]^{2/5}\right\}^{-1/4} \quad (9)$$

(cf. Blandford and Rees 1974). If $p_e(z)$ is a monotonically decreasing function of z, then $r(z)$ first decreases and then increases with z, attaining a minimum at the position z_n of the nozzle:

$$r_n = 0.4 L_w^{1/2} V_w^{-1/2} p_0^{-1/2}. \quad (10)$$

In order for the one-dimensional flow approximation to be self-consistent, it is necessary that $r_n/R_0 \ll 1$, or equivalently that $R_w/R_0 \ll 0.85$. If the bubble is in pressure equilibrium with the surrounding medium, then buoyancy forces associated with the gravitational field of the central star will tend to maximize the ratio R_w/R_0 (Smith *et al.* 1981); however, when the bubble is still decelerating, this effect may be suppressed (see § III*a*). Smith *et al.* (1981), who analyzed the stability of the stationary nozzle configuration, found that it will be disrupted by the Kelvin-Helmholtz instability if the ratio r_n/z_n is too small. Since for a power-law pressure distribution z_n is of order R_0, this conclusion also suggests that $r_n \sim R_0$. For a nearly isotropic distribution of the form $p_e(R) = BR^{-n}$ $(n < 2)$, one can determine R_0 from this condition, using equation (10). (Note, however, that in this case the one-dimensional flow approximation may not be too accurate.) The value of R_0 can be bracketed by the mass and energy conservation relations which are postulated in this model. The inequality $\dot{M}_{ev}/\dot{M}_{out} < 1$ provides an upper limit, which is numerically the same as the one given for R_t in § II. A lower limit on R_0 is imposed by the adiabatic approximation, which requires the flow time between the shock and the nozzle ($\sim R_0/V_w$) to be shorter than the radiative cooling time of the shocked wind. A calculation similar to the one leading to equation (7) gives $R_0 \gtrsim 10^{12}(L_w/L_\odot)(V_w/10^3 \text{ km s}^{-1})^{-7.2}$ cm. Note that this limit is much lower than R_t (eq. [7]); this reflects the fact that the velocity V_s, which determines the dynamical time scale of an expanding bubble, is much smaller than V_w. This also suggests that the flow pattern discussed here could develop, under suitable conditions (e.g., if the outer shell is accelerating; see § III*a*), also in a momentum-driven interstellar bubble.

In order for a stationary nozzle configuration to be achieved, it is necessary that the exponent n in the external distribution be smaller than 2, since the ram pressure of the wind falls as R^{-2} (Smith *et al.* 1981). However, it is conceivable that a quasi-stationary configuration could still be established even when the bubble is not in pressure equilibrium with the ambient medium, provided that the lateral expansion velocity of the cavity walls is much smaller than V_w. In this case the nozzles would be supported by ram pressure rather than by the static external pressure. We can estimate the evolution of the stagnation radius R_0 when $p_e(R_0) \ll p_0$ from equation (3), in which m is now interpreted as the exponent of the density distribution in the equatorial plane, after multiplying the right-hand side by $[(3/4)(16/15)^{5/2}]^{1/(4-m)}$ to take account of the fact that the shocked stellar wind is compressed adiabatically rather than radiatively. The evolution of the jet radius for $z < z_n$ is similarly determined by the external density distribution. For example, in the special case $\rho_e(r, z) = A(z)r^{-m}$, the simplest solution in the one-dimensional-flow approximation is a quasi-homologous expansion of the entire cavity-nozzle structure, with $r(t) \propto R_0(t)$ and $p(z) \propto A(z)r(z)^{2-m}$. The function $r(z)$ can be obtained by substituting $p(z)$ into equation (9), and may describe a transonic convergent-divergent nozzle if $A(z)$ decreases monotonically with z. The position of the nozzle is determined as before by the condition $p_n = 0.49p_0$; hence, this simple solution is self-consistent only for $R_0 < z_{max}$, defined by $A(z_{max}) = 0.49A(0)$. It is conceivable, however, that supersonic jets would form in an interstellar bubble which became unstable to the formation of nozzles even if a convergent-divergent flow pattern could not be maintained. One possibility in this case is that the wind shock would become discontinuous near the symmetry axis, thus creating two effective nozzles. However, since the jets in this picture comprise only that part of the original flow which was directed toward the nozzles, this configuration would be much less efficient in tapping the kinetic power of the wind.

In the collapsing isothermal sphere model (Shu 1977) which was outlined in § III*a*, the pressure distribution is a power law in radius with exponent $n = 5/2$ in the free-fall zone, and $n = 2$ in the hydrostatic envelope. It follows that an interstellar bubble which expands into a protostellar environment that is described by this model cannot be confined by static pressure alone. However, the actual pressure distribution in molecular clouds may well be anisotropic, due, for example, to the presence of embedded magnetic fields. This behavior is apparent in

the isothermal equilibrium models constructed by Mouschovias (1976), in which the steepest pressure gradient always occurs along the magnetic field lines, although the precise form of the distribution differs from cloud to cloud and depends on initial and boundary conditions. In such clouds the lateral magnetic stresses could help confine the bubble and maintain a stationary nozzle configuration.

c) *Propagation Effects*

After the jets are established at the nozzles as a directed supersonic outflow, they can be collimated by pressure forces as they propagate through the ambient medium. This effect is discussed in detail in a recent review paper (Begelman, Blandford, and Rees 1982), and here we only summarize the main results. The condition for pressure confinement (which is also the condition for the one-dimensional flow approximation to remain valid) is $(dp_e/dz) < (C_s/V)(dr/dp_e)^{-1}$, where C_s is the internal sound speed of the jet and (dr/dp_e) is given from equation (9). In the supersonic regime where $V \approx V_w =$ const, the density and pressure in the jet scale as $\rho \propto r^{-2}$ and $p \propto r^{-2\Gamma}$, respectively, where $\Gamma = 5/3$ for an atomic gas and $\Gamma = 7/5$ for a molecular gas. For an external pressure distribution of the form $p_e(z) = Bz^{-n}$, $rV/zC_s \propto z^{(n-2)/2}$, and the condition for pressure confinement is simply $n < 2$. The effective opening angle of the jet, $\theta_{\rm eff} = 2r/z$, scales as $z^{(n-2\Gamma)/2\Gamma}$ in this case, whereas a free jet expands with a constant opening angle. Thus the degree of collimation in a confined jet is increased relative to that of a free jet if n is smaller than 2Γ. For example, if $z_n = 2r_n$, $n = 1$, and $\Gamma = 5/3$, then at $z = 10z_n$, $\theta_{\rm eff} = 11.^\circ 4$; $\theta_{\rm eff}$ increases for smaller values of Γ and for larger values of n.

If the pressure changes so rapidly at some point along the jet that the condition $dr/dz < (C_s/V)$ is locally violated, then even though the jet becomes confined again, a basically two-dimensional flow pattern is set up and propagated downstream. An extreme example of this behavior is that of a supersonic jet emerging from a rigid channel into a uniform region of lower pressure (e.g., Courant and Friedrichs 1948). The flow pattern in that case is shown schematically in Figure 3: the jet tries to accomodate to the reduced external pressure by expanding sideways, but instead it "overshoots" and reconverges, initiating a series of oscillations which continue until the action of viscosity damps them out. The oscillations in radius are accompanied by potentially large pressure gradients along the axis of the jet: the pressure is maximized at the narrowest point, where its value p_1 exceeds the ambient pressure p_2, and it is minimized at the widest point, where its value p_3 is less than p_2. The flow can be analyzed by the method of characteristics in terms of a stationary configuration of alternating rarefaction and compression waves. (In practice, the converging compression waves near the center of the jet steepen to form shocks, the so-called Mach disks, where energy is dissipated.) In the case of a purely two-dimensional flow, the deflection angle of the stream across such a wave, δ_{ij} (from point i to point j),

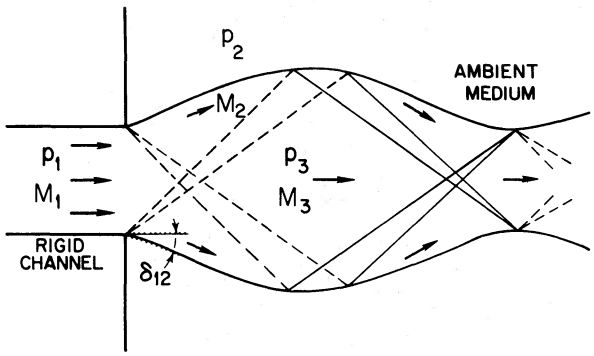

FIG. 3.—Schematic flow pattern of a supersonic jet which emerges with pressure p_1 and Mach number M_1 from a rigid channel into a uniform medium with pressure $p_2 < p_1$. The induced oscillations in the jet's cross section can be described in terms of a succession of stationary rarefaction (---) and compression (——) waves. At the widest point the pressure on the axis is $p_3 < p_2$, and the corresponding Mach number is $M_3 > M_2 > M_1$. The arrows indicate the direction of the flow, and δ_{12} denotes the deflection angle of the boundary at the exit from the channel.

can be given in advance of any particular flow problem in terms of the Mach number M_i ($M \equiv V/C_s$) and the pressure ratio $\xi = p_j/p_i$. Specifically,

$$\delta_{ij} = \epsilon(M_j) - \epsilon(M_i)\,, \tag{11a}$$

where

$$\epsilon(M) = \left(\frac{\Gamma+1}{\Gamma-1}\right)^{1/2} \arctan\left[\left(\frac{\Gamma-1}{\Gamma+1}\right)(M^2-1)\right]^{1/2} - \arctan\,(M^2-1)^{1/2} \tag{11b}$$

and

$$M_j = \{1/(\Gamma-1)[(\Gamma-1)M_i^2+2](\xi^{(1/\Gamma-1)}-2)\}^{1/2} \tag{11c}$$

(e.g., Courant and Friedrichs 1948). In particular, equation (11) can be used to calculate the initial deflection angle of the boundary, δ_{12} (for given values of M_1 and p_2/p_1), and the pressure ratio p_3/p_2, which is found after M_3 is deduced from the condition $\epsilon(M_3) = 2\epsilon(M_2) - \epsilon(M_1)$. For example, for $M_1 = 5$, $p_2/p_1 = 1/5$, and $\Gamma = 5/3$, these relations imply $\delta_{12} \approx 9^\circ$ and $p_1/p_3 \approx 57$. (The deflection angle and p_1/p_3 decrease with increasing M_1 and p_2/p_1.) The behavior of an axisymmetric jet is similar to that of the purely two-dimensional one, although its structure depends on the specific flow problem and must be calculated numerically. One can estimate the wavelength of the oscillations in such a jet from linear theory as $l = 2.6(M_1^2-1)^{1/2}r_1$, where r_1 is the radius of the channel (e.g., Pai 1953), but this estimate is strictly valid only for $1 \ll M_1^2 \ll (dr/dz)^{-1}$. The exact shape of an oscillating jet will, of course, deviate from the structure considered in Figure 3 when the external pressure changes less abruptly, or when the initial streamlines are not parallel. However, the two-dimensional flow pattern, manifested in quasi-periodic oscillations in r and p, is expected to remain qualitatively the same, and has indeed been seen in numerical simulations of

jets which pass between regions of different pressure distributions (e.g., Chan and Henriksen 1980). This flow pattern may be relevant to various observed phenomena in bipolar sources. The quasi-periodic "Mach disks" along the jet, which are sites of shock dissipation, could be perceived as emission knots and identified with Herbig-Haro objects. For example, the roughly collinear and quasi-regularly spaced Herbig-Haro objects HH 7–11, strung out along the bipolar CO lobes in NGC 1333 (Snell and Edwards 1981), could be produced by this effect. (Note that in this interpretation the emission sites should show no systematic proper motions; the nature of Herbig-Halo objects with directed proper motions is discussed in § III*d*.) The oscillations of the boundary of a supersonic jet which are induced by a change in the external pressure could explain the apparent flaring up of the optical jet associated with IRS 5 (Strom, Grasdalen, and Strom 1974), and may be relevant also to the interpretation of fan-shaped cometary nebulae (e.g., Cohen 1973, 1974) and of bipolar nebulae in general (e.g., Calvet and Cohen 1978). In these cases the expansion might be triggered by the emergence of the jet from a dense cloud or core of a cloud [where $p(R) \propto R^{-2}$, say, if the collapsing isothermal sphere model is applicable] into the intercloud or intracloud medium, where the pressure distribution is less steep. The subsequent reconvergence of the boundary, as well as the fact that the infrared object associated with these sources is, in several cases, significantly offset from the apex of the nebula (Cohen 1973), find a natural explanation in this picture. The morphology of these nebulae could, alternatively, be interpreted in terms of an interstellar bubble expanding in an anisotropic medium (see Fig. 1). This interpretation was previously suggested in models where the cavity was assumed to form by the direct impact of the stellar wind (e.g., Barral and Cantó 1981). In the context of the jet model, however, the bubble could also be identified with the hot "cocoon" that may form out of shocked jet material, as discussed below. That the morphology of at least some of these nebulae is associated with fast outflows from young stars is suggested, for example, by the presence of deep P Cygni absorption profiles, broad emission-line wings, and rapid structural changes in a source like PV Cep—a fan-shaped cometary nebula associated with a highly reddened T Tauri star (Cohen *et al.* 1981). (Outflowing winds have been inferred to exist also in the nuclei of planetary nebulae [e.g., Mathews 1966], which supports the idea that the bipolar structures which are observed in many of these sources [e.g., Schmidt and Cohen 1981] are produced by the same processes that operate in the vicinity of "bipolar" pre-main-sequence stars.) Observational support for the interpretation of bipolar nebulae in terms of the same general mechanism which gives rise to bipolar CO emission lobes and aligned Herbig-Haro objects is provided by a source like R Mon (Cantó *et al.* 1981), where all of these features have been detected in the vicinity of the embedded infrared object. The possible link between bipolar nebulae and jets is supported by the recent detection of a distinct Hα jet along the axis of the cometary nebula 1548C27 (Craine, Boeshaar, and Byard 1981).

The radial oscillations that we have considered could be regarded as a flow instability which is excited by a pressure perturbation at the boundary of the jet. The jet would also be subject to other types of instability, in particular the Kelvin-Helmholtz instability (e.g., Hardee 1979), which could modify its structure and possibly even lead to its disruption. A Kelvin-Helmholtz instability would, however, only affect a confined jet, and its growth rate is considerably reduced if the jet is highly supersonic. Furthermore, in a dense medium, the growth rate of certain modes would be reduced also by the accumulation of ambient material after the motion of the boundary became supersonic (see Benford 1981). Even if the jet is disrupted, it could be recollimated in an external pressure or density gradient, with the process conceivably repeating in a quasi-periodic fashion (Sparke 1982; see also Chan and Henriksen 1980). This may provide an alternative interpretation of Herbig-Haro objects such as HH 7–11 if, again, they are stationary.

The heads of the jets, where the flow is decelerated by the impact on the ambient medium, have the same general structure (namely, inner and outer shocks separated by a contact discontinuity) as the outer regions of an interstellar bubble. The intercepted external medium passes through the outer radiative shock and is partially swept up, the rest being deflected sideways by the advancing head. The accumulated material moves with a velocity $V_h \sim [\rho_j(z_h)/\rho_e(z_h)]^{1/2} V_j$, where the subscripts h and j refer to the head and jet, respectively (see eq. [4]). Substituting $\rho_j(z_h) = 8L_j/\pi\theta_{\rm eff}{}^2 z_h{}^2 V_j{}^3$, and scaling by typical parameters, we obtain

$$V_h \sim 9.4 \left(\frac{L_j}{L_\odot}\right)^{1/2} \left(\frac{z_h}{0.1\ \mathrm{pc}}\right)^{-1} \left(\frac{\theta_{\rm eff}}{30^\circ}\right)^{-1} \left(\frac{V_j}{10^3\ \mathrm{km\ s^{-1}}}\right)^{-1/2} \times \left(\frac{\rho_e}{10^{-21}\ \mathrm{g\ cm^{-3}}}\right) \mathrm{km\ s^{-1}}\ . \quad (12)$$

The heads (or "working surfaces," in the terminology of Blandford and Rees 1974) could be identified with the two oppositely directed, high-velocity CO emission-line lobes described in the Introduction. We expect that similar bipolar emission patterns would show up also in high-sensitivity observations of other molecular lines. In fact, observations of H_2 (Beckwith *et al.* 1978; Nadeau and Geballe 1979), SiO (Downes *et al.* 1982), and SO (Plambeck *et al.* 1982) have already provided evidence for a bipolar outflow in Orion-KL, and an NH_3 map of L1551 (Torrelles *et al.* 1981) has revealed an elongated feature aligned with the high-velocity CO lobes. Part of this emission could also originate in shocked jet material which has cooled and accumulated in the heads (see Chernoff, Hollenbach, and McKee 1982). If, however, the cooling time behind the inner shock exceeds Z_h/V_h, then the shocked jet material would create a hot "cocoon" around the jet (e.g., Scheuer 1974; Norman *et al.* 1981*b*), whose pressure would act to confine the jet laterally, as well as to drive a sideways expansion

of the outer boundary. As long as this pressure is lower than the ram pressure at the heads, the cocoon will be spindle-shaped even if the external density distribution is isotropic. However, if the solid angle subtended by the jets is sufficiently large (roughly, $\theta_{\rm eff}{}^2 > [\rho_j(z_h)/\rho_e(z_h)]^{1/2}$; see Scheuer 1974), then the entire cavity would evolve as an energy-driven interstellar bubble (see eq. [6]).

The interpretation of the motion of bipolar emission lobes in terms of anisotropic outflow clearly reduces the energy and momentum requirements at the central source as compared with the values deduced on a spherical-outflow model. (The reduction factor is roughly $\frac{1}{8}\theta_{\rm eff}{}^2$, which for L1551 is $\sim$0.03, if we identify $\theta_{\rm eff}$ with the angle between the velocity vectors of HH 28 and HH 29.) The momentum discharge from the central source can be estimated, in the case of a momentum-driven shell, from the force $\sim M_s V_s{}^2/R_s$ acting on the shell. As was noted, e.g., by Lada and Harvey (1981), in many bipolar CO sources the momentum discharge inferred in this way is much larger than L_*/c, the momentum injection rate to a radiatively driven, optically thin stellar wind. The discrepancy can in some cases be traced to the fact that the force acting on the shell was overestimated by assuming spherical symmetry. However, in a number of sources, including L1551 (Snell, Loren, and Plambeck 1980), the discrepancy persists even after anisotropic mass distribution in the shell is taken into account. In this particular source the problem would be resolved if the shell were energy-driven (rather than momentum-driven), since the inferred momentum injection rate would then be reduced by a factor $\sim V_s/V_w$. Other possibilities are that the wind is optically thick, in which case the momentum injection rate is increased by a factor of order the optical depth (Phillips and Beckman 1980), or that the wind is not radiatively driven, although some of the alternative driving mechanisms that have been proposed for low-mass stars are also not expected to yield momentum injection rates which are as high as the largest driving forces that have been deduced (see DeCampli 1981).

d) Acceleration of Condensations by the Jet

We now turn our attention from the large-scale interactions of the flow with the ambient medium, which determines the global properties of the jet, to the small-scale interaction with local density inhomogeneities. A high-velocity jet which encounters a stationary condensation (whose size is much smaller than the radius of the jet) will accelerate it downstream by the ram pressure of the flow. As long as the relative velocity between the jet and the clump is supersonic, the incident flow will be decelerated in a strong bow shock, although the shocked fluid can be reaccelerated further downstream. Initially, another shock will be driven into the clump (e.g., McKee and Cowie 1975), bringing it into pressure equilibrium with the shocked incident flow. At the end of this initial phase the clump may fragment (as a result of the Rayleigh-Taylor and Kelvin-Helmholtz instabilities at the contact discontinuity with the shocked jet), and each of the resulting subcondensations could then be accelerated independently. The detailed evolution of such clumps has been treated by several authors (e.g., McKee, Cowie, and Ostriker 1978; Schwartz 1978; Blandford and Königl 1979*a*, *b*), and here we only summarize the results which are relevant to the present application. The clump is characterized by its velocity V_c, adiabatic index Γ_c, density ρ_c, scale height h, and mass $M_c \propto \rho_c h^3$. If the density in the jet varies with distance from the origin as $\rho_j(z) \propto z^{-q}$, then the equation of motion for the condensation is

$$\frac{dy}{dx} = ay^{-1}(1-y)^u x^{-(qu/2)}, \tag{13}$$

where $y = V_c/V_j$, $x = z/z_0$, $a = C\rho_{j0} z_0 h_0{}^2 M_c{}^{-1}$, and $u = 2(3\Gamma_c - 2)/3\Gamma_c$. Here the subscript zero denotes the initial parameters of the cloud, and the constant C depends on Γ_c, Γ_j, and on the specific model adopted for the clump. (For example, in the isothermal model of De Young and Axford 1967, $C = 6.49$ for $\Gamma_c = \Gamma_j = \frac{5}{3}$.) The solution of equation (13) for u different from 1, 2, or $2/q$ is

$$\frac{1}{(2-u)(u-1)}\{(1-y)^{1-u}[1-(u-1)y]-1\} = \frac{2a}{2-qu}[x^{(2-qu)/2}-1]. \tag{14}$$

Hence, for $u > 1$ (i.e., $\Gamma_c > \frac{4}{3}$), the clump will attain the velocity of the jet only if $q < 2/u$; for larger values of q the asymptotic velocity $V_{c\infty}$ will be less than V_j, although the difference will be small if the acceleration parameter a is large. In a free jet, $q = 2$, and so $V_{c\infty} < V_j$, whereas in a jet confined by an external pressure $p_e(z) \propto z^{-n}$, $V_{c\infty} = V_j$ if $n < 2\Gamma_j/u$. Since the condition for confinement in this pressure distribution is $n < 2$, it follows that a clump accelerated by a confined jet will always attain the jet velocity for typical values of Γ_j and Γ_c ($\frac{5}{3}$ or $\frac{7}{5}$). In the derivation of equation (13) it was assumed that an accelerated clump expands adiabatically as it moves downstream. The increase of the scale height h with distance is given by

$$h = h_0(1-y)^{-(2/3\Gamma_c)}x^{(q/3\Gamma_c)}. \tag{15}$$

In a free jet, h increases more slowly with z than the jet radius, and this is also true initially in a confined jet. However, for $z \gg z_0$, the scale height in a confined jet increases as $z^{(2-q)/(3\Gamma_c-4)}(\Gamma_c > \frac{4}{3})$, and in general grows faster with z than $r(z)$. (This conclusion holds only so long as the jet remains supersonic with respect to the clump.)

An accelerated-clump model similar to the one discussed here has been proposed for Herbig-Haro objects by Schwartz (1978), who more recently demonstrated that many spectral characteristics of HH 1 in particular could be explained in terms of the emission from the bow shock and the cloud shock expected on this model (Schwartz 1981; see, however, Böhm, Böhm-Vitense, and Brugel 1981 for a discussion of some

apparent difficulties with the shock interpretation). In the original picture, the clumps were interacting with an isotropic wind, which led to an inferred kinetic luminosity for the wind in excess of the bolometric luminosity of the associated infrared source (Cohen and Schwartz 1979). However, as was noted by several authors, this difficulty can be alleviated if the outflow is anistropic. Such an outflow is a natural consequence of the jet picture (see Cantó and Rodríguez 1980 for a similarly motivated scheme). Additional support for the jet interpretation for HH 1 and HH 2 (which lie on opposite sides of the exciting star and are almost collinear with it) comes from proper-motion measurements (Herbig and Jones 1981), which show that each of these objects is composed of a number of subcondensations that move with large and disparate speeds, but whose velocity vectors almost always point away from the central star. A similar conclusion regarding the direction of the velocity vectors has been reached for HH 28 and HH 29, which move away from IRS 5 in L1551 (Cudworth and Herbig 1979), and for the nuclei of HH 39, which move away from R Mon (Herbig and Jones 1981). In the context of the jet model, the clumps could be interpreted as portions of the jet's wall which were torn off by the Kelvin-Helmholtz instability, and entrained in the stream. This effect is most likely to occur in the vinicity of the nozzle, and has been noted in numerical simulations (Norman *et al.* 1981*a*). Another possibility is that the condensations have formed as a result of a thermal instability in the subsonic region of the nozzle, which decoupled them from the rest of the accelerating flow. Alternatively, the condensations could be part of the intracloud medium (see, e.g., Larson 1981 for a discussion of the clumpy structure of interstellar clouds) which either lay in the path of the jet or which moved into the flow (see § IV*c* in Blandford and Königl 1979*b*).

HH 1 and HH 2 could be examples of clumps which first encountered the jet near their present locations, and which are still in the process of fragmentation as they come into pressure equilibrium with the flow. Note that the equilibration time scale, $\sim(\rho_{c0}/\rho_{j0})^{1/2}h_0/V_j$, is shorter than the acceleration time scale by a factor $(\rho_{j0}/\rho_{c0})^{1/2}$, which could be quite small when $\rho_{c0}/\rho_{j0} \gg 1$. In order to estimate these parameters in HH 1, we adopt $h_0 \sim 10^{16}$ cm (for an assumed distance of 500 pc), and $\rho_{c0} \sim 2 \times 10^{-20}$ g cm^{-3} (Elias 1980). The fastest subcondensation in this object has a proper motion of ~ 350 km s^{-1} (Herbig and Jones 1981), whereas the shock model for the spectrum (Schwartz 1978) implies a relative velocity between the jet and the clump of ~ 100 km s^{-1}; hence, we adopt $V_j \sim 500$ km s^{-1}. The shock model also implies $\rho_{j0} \sim 6 \times 10^{-22}$ g cm^{-3}. The equilibration time scale is then ~ 10 yr, which is consistent with the observed fragmentation time scale (Herbig and Jones 1981). The acceleration time scale for the entire clump is a factor of ~ 6 larger, but individual fragments would be accelerated more rapidly, and could already be moving at nearly their asymptotic velocities. If the subcondensations all have roughly the same initial density, then, since the acceleration scales as h_0^{-1} and the power dissipated in the bow shock scales as h_0^2 (e.g., Blandford and Königl 1979*a*), the smaller clumps would be expected to move faster and be less luminous, although in practice these correlations may be washed out by local inhomogeneities. The opposite effect (namely, smaller objects are slower and less luminous) is expected if the condensations are decelerating (cf. Norman and Silk 1979), as may occur when clumps that have been accelerated by the flow plunge into the dense medium ahead of the jet. Other potentially observable phenomena which may serve to distinguish decelerating clumps from accelerating ones are the location of the external shock (facing downstream rather than upstream), and the relation between the full width and the degree of excitation in the spectral lines (Schwartz 1981). The Herbig-Haro object HH 3, which lies about 8 times farther away from the infrared source than HH 1 and in the same general direction, but which shows no measurable proper motion (Herbig and Jones 1981), could be an example of a clump that was brought to rest but that is still visible because the radiative cooling time (see § II) of the shocked ambient material is longer than the deceleration time. (Note that, formally, the ratio of the deceleration time scale to the cooling time scale, $\sim 10^{36} h_\infty \rho_{c\infty} V_{c\infty}^{-4.2}$, is independent of the ambient density.) It is conceivable, however, that the jet itself extends all the way out to the vicinity of HH 3, so that the head of the jet has long ago moved away from the present location of HH 1. In this case, if HH 1 and HH 2 represent dense blobs that have only recently encountered the flow, then they probably did not lie along the original trajectory of the jet, but rather entered the flow as a result of their own motion in the cloud or of the sideways motion of the jet.

An alternative interpretation of Herbig-Halo objects with systematic proper motions is that they are shocks which propagate on their own along the jet, without being attached to dense clumps. Such shocks could evolve from fluctuations in the flow velocity which are induced near the origin of the jet (Rees 1978). However, unlike the accelerating-clumps model, there is no natural interpretation of the observed infrared spectra in this case (cf. Schwartz 1981), and it is also difficult to account for the morphology of objects like HH 1 and HH 2, especially in view of the fact that shocks which propagate in the direction of decreasing density are not subject to the Rayleigh-Taylor instability.

IV. FORMATION OF BIPOLAR SOURCES IN MAGNETIZED MOLECULAR CLOUDS

a) Dynamical Effects

In § II we noted that the presence of an ordered ambient magnetic field could indirectly influence the expansion of an interstellar bubble through its effect on the external density distribution. The fact that the density gradient is steepest along the magnetic field lines is apparent in the equilibrium models of self-gravitating, magnetized clouds which were studied by Mouschovias (1976), and which may also represent clouds in a state of quasi-static contraction. A self-gravitating cloud with an

initially uniform magnetization is not expected to have an isotropic density distribution except in its densest regions, where ambipolar diffusion has increased the mass-to-flux ratio above the critical value for gravitational collapse (e.g., Mouschovias 1978), a situation which probably prevails only in the immediate vicinity of a protostar. The ambient magnetic field would also affect the expansion directly through the action of magnetic stresses on the boundary. However, these effects would be relatively unimportant as long as the expansion speed of the outer shell is much larger than the Alfvén speed in the ambient medium. Now, the magnetic field B_e in the core of the cloud is expected to scale with a power of the density ρ_e which is not larger than $\frac{1}{2}$ (Mouschovias 1976). Hence, the Alfvén speed $V_{Ae} = B_e/(4\pi\rho_e)^{1/2}$ would at best remain constant during the contraction of the cloud, and in practice would probably decrease. The same conclusion applies also before the cloud becomes self-gravitating. We can therefore set an upper limit on V_{Ae}, using the more accessible parameters of the intercloud medium. Even for a magnetic field as large as 3 microgauss at a density of 1 cm^{-3}, this upper limit (5.7 km s^{-1}) is substantially smaller than the observed velocities of molecular emission-line sources ($\gtrsim$15 km s^{-1}). It is conceivable, however, that the observed velocities correspond to motion along the magnetic field lines, and that other parts of the outer shell have lower velocities and are strongly affected by the magnetic stresses. To illustrate this possibility, we consider an idealized example of an energy-driven interstellar bubble expanding in a magnetically dominated medium with a uniform magnetic field B_0 in the z-direction, and a density distribution $\rho_e(z) = Az^{-m}$ $(0 \leq m < 2)$. The initial evolution of the bubble can be approximated by equations (A3)–(A5) in the Appendix. Eventually, after the internal pressure drops to the value of the ambient magnetic pressure, the transverse motion of the bubble is halted, and the circumferential shell is dispersed. However, the expansion at small angles to the field lines continues virtually unimpeded, so the bubble elongates along the z-axis even if m is small. The bubble can therefore be approximated by a thin cylinder of radius R and height $2Z$. The subsequent evolution can be estimated by requiring that pressure balance be maintained across the side walls. In the limit $R^2/Z^2 \ll 1$, this condition is $p \approx B_0^2/8\pi$, which gives $Z \propto t^{2/(2-m)}$, $R \propto t^{-m/(4-2m)}$ (eq. [A8] in the Appendix). In particular, for $m = 0$, the main body of the bubble maintains roughly a constant radius, and elongates at a rate $2^{1/2}V_{Ae}$ (cf. Levy 1971). For $m \neq 0$ we expect that, in a real cloud, the magnetic field itself would decrease away from the plane $z = 0$. In that case, the elongation velocity of the bubble would exceed $V_{Ae}(Z)$ by a factor $\sim B_e(0)/B_e(Z)$.

The magnetic field which is trapped in the swept-up material will affect the shape of the outer shell, and, to some extent, also its motion. These effects are important when the magnetic pressure in the shell exceeds the local thermal pressure. For propagation at a right angle to the field lines (subscript $\perp$), this occurs when the temperature in the shell drops below $T_m = 3.8 \times 10^3$ $(V_s/15$ km s$^{-1})$ $(V_{Ae}/5.7$ km s$^{-1})$K [Hollenbach and McKee 1979; these authors estimate that the results for normal propagation are accurate, to within 30%, for angles larger than $\tan^{-1}(5V_{Ae}/V_s)$]. In this case (and for $V_s \gg V_{Ae}$), the density in the shell is $\rho_{s\perp} \approx (2^{1/2}V_s/V_{Ae})\rho_e$. On the other hand, for propagation at a small angle to the field direction (subscript $\|$), the thermal pressure in the shell remains larger than the magnetic pressure, and the density is given by $\rho_{s\|} \approx (V_s/C_s)^2\rho_e$. (This approximation is valid when both the internal isothermal sound speed C_s and the external sound speed C_{se} are much smaller than V_s.) For a shell expanding in a dense molecular cloud, the temperature of the shocked, swept-up material drops rapidly to its final value of 50–150 K, which should be roughly uniform around the shell. [The cooling time would be roughly independent of the location in the shell even though the cooling rate ($\propto\rho_s^2$) is lower in regions which move at a large angle to the field, because in these regions the postshock temperature and heat input are also reduced; e.g., Field *et al.* 1968.] Since this value is typically much smaller than T_m, we expect that for a nearly uniform ambient medium, $\rho_{s\|} \gg \rho_{s\perp}$, and therefore that the shell would be much thicker near the equator than at the poles. The exact structure of the shell is difficult to calculate (see Giuliani 1982), but qualitatively we expect that it has the shape shown schematically in Figure 4. In this picture, the magnetic stresses in the shell cause its inner boundary to become spindle-shaped (cf. Levy 1971 and Heiligman 1980), while at the same time causing the outer shock to slow down in the polar regions and to speed up in the equatorial plane, relative to the velocity in the absence of a magnetic field. The latter behavior was found by Kulsrud *et al.* (1965) in the case of a perfectly conducting, spherical piston which expands super-Alfvénically into a uniformly magnetized medium. However, even in the original problem this effect was quite small, and it is probably even smaller in the present case, where the "piston" is not solid. Therefore, in a typical dense cloud, this effect would probably be dominated by the influence of the induced external density gradient, resulting in an overall elongation of the outer shock in the direction of the ambient field.

b) Radiative Effects

Even if the dynamical effects of the magnetic field—both direct (magnetic stresses) and indirect (induced anisotropic density distribution)—do not lead to significant departure of the bubble's shape from sphericity, it is still possible that the anisotropic internal density distribution which is established when parts of the shell become magnetic-pressure dominated (§ IV*a*) could give rise to an *apparent* bipolar molecular emission pattern in the presence of a strong central UV source. To illustrate this effect, we consider a spherical bubble which expands in a homogeneous medium of atomic-hydrogen density n_0 and magnetic field B_0. We assume that the thickness of the dense outer shell always remains small compared to the radius R_s, and that it can be approximated as having a uniform total pressure. As was discussed in § IV*a*, the density $n_{\|}$ in those regions of the

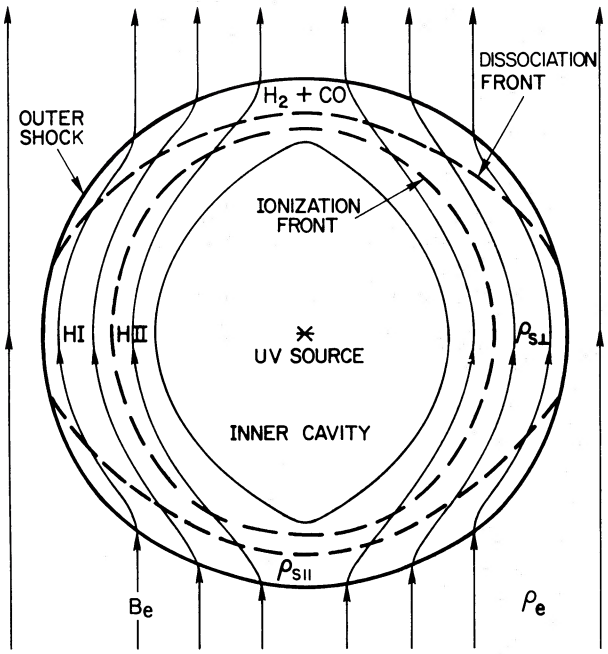

FIG. 4.—Schematic structure of the outer shell of an interstellar bubble which expands in a medium with density ρ_e and magnetic field B_e. In this diagram it is assumed that the external density and pressure distributions are isotropic, so that the shell is roughly spherical. (The thickness of the shell is, however, highly exaggerated in this figure.) Because of magnetic pressure effects, the density $\rho_{s\parallel}$ in the polar regions of the shell could greatly exceed the density $\rho_{s\perp}$ in the equatorial plane. In the presence of a central UV source which drives ionization and dissociation fronts into the shell, these variations in the internal density could give rise to a bipolar distribution of H_2 and CO.

shell which move at a small angle to the field lines could be much larger than $n_{s\perp}$, the density in the magnetic-pressure-dominated regions of the shell, if $V_s \gg C_s^2/V_{A0}$. However, the total column density of swept-up material, $N_s = n_0 R_s/3$, is, by our assumptions, independent of position in the shell. In addition, we assume that the central object is a strong source of UV photons with luminosity L_{UV}. These photons will initially dissociate the molecules and ionize the atoms ahead of the expanding bubble, but eventually the ionization and dissociation fronts will be overtaken by the shell and trapped inside it (Hollenbach, Chu, and McCray 1976). The radius R_i at which the ionization front is trapped can be estimated (cf. Weaver *et al.* 1977) by setting $L_{UV} \exp(-KN_s) = (4/3)\pi R_i^3 \alpha^{(2)} n_0^2 (n_s/n_0)$, where $K \approx 10^{-21}$ cm^2 is the UV dust opacity, $\alpha^{(2)}$ is the radiative recombination coefficient for hydrogen, and where n_s is evaluated under the assumption that the shell is fully ionized. After the H II region is trapped, it remains confined to a thin layer at the inner boundary of the shell, of density n_{IIs} (corresponding to a speed of sound $C_{sII} \approx 10$ km s^{-1}), and column density $N_{IIs} = (L_{UV}/4\pi\alpha^{(2)} R_s^2 n_0)(n_{IIs}/n_0)^{-1}$ (which is typically $\ll K^{-1}$). However, photons in the energy range 11–13.6 eV penetrate ahead of the H II region and form a layer of dissociated molecular hydrogen. The column density N_{Is} of H I in this layer can be calculated as a function of the column density N_{2s} of H_2 by assuming that the photodestruction of molecules is balanced by formation on grains, and again taking into account the effect of dust absorption (see Hill and Hollenbach 1978). The assumption of molecular equilibrium is valid provided that both the photodissociation and the formation time scales are short compared with the age of the bubble. The photodestruction time scale can be approximated by $t_d \sim 1.5 \times 10^{-5} N_{2s}^{1/2} F^{-1} R_s^2 e^{KN_s}$ s, where FR_s^{-2} represents the unshielded UV photoabsorption rate for a hydrogen molecule (see Hollenbach, Chu, and McCray 1976, where the constant F is tabulated for stars of different spectral type). The formation time scale can be estimated by $t_f \sim (\mathcal{R} n_{Is})^{-1}$, where $\mathcal{R} \sim 3 \times 10^{-17}$ cm^3 s^{-1} is the formation rate coefficient of molecules on grains. In equilibrium $n_{2s}/n_s = t_d/t_f$, which can be regarded as a differential equation for $N_{Is}(N_{2s})$ whose solution is

$$N_{Is} = \frac{1}{K} \ln \left\{ 1 + \frac{2.8 \times 10^{21} F K^{1/2}}{R_s^2 n_s} \operatorname{erf}\left[(2KN_{2s})^{1/2}\right] \right\} \quad (16)$$

(Hill and Hollenbach 1978). It is seen from this expression that N_{Is} is limited by dust absorption to a few times K^{-1}, even in the presence of a strong UV source. The radius R_d at which the dissociation front is overtaken by the shell can be estimated from equation (16) by setting $N_{Is} = 2N_{2s} = 0.5N_s$ (typically $N_s \gg N_{IIs}$ at this stage). If at the time of trapping N_s is $\ll K^{-1}$ [which requires $n_s/n_0 \gg 27(n_0/10^4 \text{ cm}^{-3})(F/10^{-7} \text{ pc}^2 \text{ s}^{-1})(K/10^{-21} \text{ cm}^2)^{5/2}$], then the solution is

$$R_d \approx 0.72(n_0/10^4 \text{ cm}^{-3})^{-3/5}(F/10^{-7} \text{ pc}^2 \text{ s}^{-1})^{2/5} \times (n_s/n_0)^{-2/5} \text{ pc} . \quad (17)$$

Also, as long as $N_s \ll 10^{21}$ cm^{-2} [or, equivalently, $(n_0/10^4 \text{ cm}^{-3})(R_s/0.5 \text{ pc}) \ll 0.2$] continues to hold, equation (16) can be solved explicitly to give

$$N_{Is} \approx 8.1 \times 10^{21}(F/10^{-7} \text{ pc}^2 \text{ s}^{-1})^2 (R_s/0.5 \text{ pc})^{-4} \times (n_0/10^4 \text{ cm}^{-3})^{-2}(n_s/n_0)^{-2} \times \{[1 + 1.3(F/10^{-7} \text{ pc}^2 \text{ s}^{-1})^{-2}(R_s/0.5 \text{ pc})^5 \times (n_0/10^4 \text{ cm}^{-3})^3 (n_s/n_0)^2]^{1/2} - 1\} \text{ cm}^{-2} . \quad (18)$$

Equation (17) shows that, for $N_s \ll 10^{21}$ cm^{-2}, $R_d \propto (n_s/n_0)^{-2/5}$, so the dissociation front is first trapped in the densest regions of the shell, those which move at a small angle to the field lines. [A similar result applies to the trapping of the ionization front, since $R_i \propto (n_s/n_0)^{-1/3}$.] Equation (18) shows that, at that time, the ratio $N_{2s\perp}/N_{2s\parallel}$ of the molecular-hydrogen column densities for normal and parallel propagation is approximately $(2n_{s\perp}/n_{s\parallel})^2 \approx (8C_s^4/V_{A0}^2 V_s^2)$, which is typically much less than 1. This ratio could be even smaller since the column density in the shell may be below the value required for the re-formation of molecular hydrogen in the transverse direction. [The condition $t_f < R_s/V_s$ can be expressed as $N_s > 1.7 \times 10^{22} (V_s/15 \text{ km s}^{-1})(n_s/n_0)^{-1}$

cm^{-2}.] Since the CO layer in the shell is expected to roughly coincide with the H_2 layer (Glassgold and Langer 1975; Hill and Hollenbach 1978), it follows that, if the dissociation front were first trapped when $N_s \ll 10^{21}$ cm^{-2}, there would be a subsequent stage during which the column density of CO would be much larger in regions moving parallel to the field lines than in regions which move at large angles to the field. This is illustrated schematically in Figure 4. Under these circumstances, the intensity of optically thin CO rotational transition lines (which is proportional to the column density of CO) would vary around the shell in an apparent bipolar pattern. This effect would diminish after N_s came to exceed K^{-1}, and if the lines became optically thick. (Note that a similar radiation pattern is not expected from the trapped H II region, because the emission measure $EM = 2n_{\rm IIs}N_{\rm IIs}$ is independent of $n_{\rm IIs}$.) The ratio $N_{2s\perp}/N_{2s\parallel}$ is expected to be further reduced in shells which expand preferentially in the direction of the ambient field, since in that case the regions which move at large angles to the field lines would be relatively closer to the central object, and would therefore be exposed to a larger flux of dissociating photons. Thus, the radiative effect induced by a strong UV source may enhance the kinematic effect of anisotropic expansion in producing a bipolar emission pattern in a cloud with an ordered magnetic field. Which of these two effects is dominant in a given source could in principle be determined by sampling the emission-line profiles around the shell, since an anisotropic expansion would give rise to strong variations in the *width* of the broad wings, whereas a dissociation front trapped inside a spherical shell would manifest itself mainly by changes in the *intensity* of the wings. Although in practice it may be difficult to separate the two effects, one might still be able to infer the presence of a strong UV source from other observations. For example, in the case of GL 490, there is direct evidence from Bγ observations (Thompson and Tokunaga 1979; Simon *et al.* 1981) for an ionizing photon luminosity $\gtrsim 10^{46}$ s^{-1}, comparable to the Lyman continuum luminosity of a B0.5 zero-age main-sequence star. The dissociating flux for such a star corresponds to $F = 2.4 \times 10^{-7}$ pc^2 s^{-1} in equations (15)–(17) (Hollenbach, Chu, and McCray 1976), which may be a fair approximation for GL 490 even if the UV flux comes predominantly from an accretion disk, or if the star has not yet reached the zero-age main-sequence (see Thompson and Tokunaga 1979). The inferred value of F will, however, be much lower if the Bγ emission region in this source is ionized primarily by Balmer continuum photons, as was suggested by Simon *et al.* (1982).

If the central star is a source of both UV photons and a spherically symmetric wind, then, in order for the ionizing photons to penetrate through the wind and reach the outer shell, their luminosity must satisfy $L_{\rm UV} > 1.4 \times 10^{41}(L_w/L_\odot)^2(V_w/10^3 \text{ km s}^{-1})^{-6}(R_*/10^{12} \text{ cm})^{-1}$ s^{-1}, where R_* is the stellar radius (e.g., Wright and Barlow 1975). Dissociating photons should generally be able to escape, since, beyond the radius R_g where grains can start to form (e.g., Draine 1979), t_f is already larger than R_g/V_w for typical parameters. However, absorption by dust could itself attenuate the UV flux in sufficiently dense winds. If the inner wind shock is radiative, then, for $V_w \gtrsim 100$ km s^{-1}, it could itself become a detectable source of UV photons; however, the dissociating flux would typically be too low to affect the radiation pattern from the outer shell (cf. Shull and McKee 1979).

c) *Observational Support*

The various effects of an ambient magnetic field in an expanding interstellar bubble that we have considered do not require very large *absolute* values for the magnetic field. Rather, they require that the magnetic energy in the cloud be sufficiently large *relative* to both the gravitational and internal energies, so that magnetic stresses can play a significant role in the dynamical evolution of the cloud. That this requirement is indeed met in the vicinity of many embedded protostellar sources is indicated by polarization measurements (e.g., Dyck and Lonsdale 1979) which find a strong correlation between the infrared polarization directions of these sources and the visual polarization directions in the surrounding interstellar medium. Since the interstellar polarization direction is believed to be controlled by the ambient magnetic field (see, e.g., Spitzer 1978), these results suggest that the magnetic field remains strong enough during gravitational collapse to maintain its original orientation. In fact, detailed observations in one dense cloud of this sort (Vrba, Coyne, and Tapia 1981) have produced an inferred empirical scaling of the magnetic field with density which is consistent with theoretical models of self-gravitating, magnetized clouds (Mouschovias 1976). As was mentioned in the Introduction, the measured visual polarization position angles in L1551 lie in approximately the same direction as the central continuum "jet," the CO lobes, and the velocity vectors of HH 28 and HH 29, and indicate a uniformly magnetized cloud. A similar alignment between CO lobes, Herbig-Haro objects, and the local polarization direction was noted in NGC 1333 (Snell and Edwards 1981) and in NGC 2068 (Snell and Edwards 1982). It is also indicated in R Mon, as can be seen by comparing the CO maps of this source (Cantó *et al.* 1981) with the polarization data for the Mon R2 region (Dyck and Lonsdale 1979). These observations therefore verify that the magnetic field is ordered on the scale of the bipolar sources, and support the hypothesis that it actually determines their orientation. (It may be relevant to mention in this connection also the statistical correlation that was found between the projected directions of the interstellar magnetic field and the major axes of planetary nebulae; e.g., Melnick and Harwit 1975.) Since in each one of the mechanisms that we have considered, the direction of elongation is *along* the local magnetic field, these results also support the interpretation of the observed polarization vectors as lying *parallel* to the magnetic field, in accord with the usual interpretation of interstellar polarization. We note that, in the case of GL 490, there appears to be a substantial

discrepancy between the direction of the CO lobes (Lada and Harvey 1981) and the mean polarization direction in the cloud (Dyck and Lonsdale 1979). However, this source also displays a high degree of circular polarization in the near-infrared ($q \sim 0.5\%$, ellipticity $e \sim 6\%$), which was interpreted as arising from a change of grain alignment along the line of sight (Lonsdale *et al.* 1980). If the direction of alignment changes uniformly by a total twist angle ϕ, then the observed position angle would be rotated by $\phi/2$ with respect to the polarization direction in the source (Martin 1974). In this model, the measured circular polarization in GL 490 corresponds to a twist angle in the range 50°–60°, depending on the adopted grain parameters (Lonsdale *et al.* 1980), which implies a polarization direction at the source close to that of the CO lobes. Since the measured polarization direction in GL 490 is parallel to the galactic plane, it is conceivable that the observed polarization is dominated by foreground grains aligned by the large-scale galactic magnetic field. In cases like this, a more accurate determination of the magnetic field structure inside the cloud would probably be obtained through CO polarization measurements (cf. Goldreich and Kylafis 1981).

The ambient magnetic field in the vicinity of molecular emission lobes can in some cases be estimated directly by fitting the observed line intensities with MHD shock models. This method has recently been applied to the Orion-KL region (Chernoff, Hollenbach, and McKee 1982; Draine and Roberge 1982), yielding preshock magnetic field strengths in the range 0.5–1.5 milligauss, and preshock densities of $2\text{–}7 \times 10^5$ cm^{-3}. These results imply that the magnetic energy density in this cloud is comparable to the gravitational energy density. Direct estimates of magnetic field strengths in regions of active star formation have been obtained also from observations of Zeeman splittings in some of the maser sources that are common to these regions. For example, a magnetic field of 3.5 milligauss was deduced in this way in an OH maser associated with Cep A, whose density was inferred to be in excess of 10^6 cm^{-3} (Wouterloot, Habing, and Herman 1980). Although these values of field and density are probably not representative of the mean values in the region where the bipolar CO lobes in this cloud are expanding (see Rodríguez, Ho, and Moran 1980), they nevertheless indicate that strong magnetic fields are present in the immediate vicinity of the embedded infrared source.

V. SUMMARY AND CONCLUSIONS

In this paper we attempted to present a unified interpretation of anisotropic emission and outflow phenomena which are detected over a wide range of scales in the vicinity of young stellar objects embedded in dense molecular clouds. Our main results can be summarized as follows:

1. An isotropic stellar wind which expands in a medium with an anisotropic density distribution would give rise to an interstellar bubble which elongates in the direction of the external density gradient.

2. Under certain conditions which are likely to prevail in protostellar environments (specifically, if the external density distribution can be approximated by a power law in radius with an exponent close to 2, and if the density and pressure distributions are at least moderately anistropic), the elongating interstellar bubble could become unstable to the formation of de Laval nozzles.

3. Once de Laval nozzles are established, the outflow becomes channeled into two oppositely directed, supersonic jets, of the type that is believed to form, on a much larger scale, near quasars and active galactic nuclei. The jets could be further collimated by a confining external pressure, as well as by their own "cocoon" of shocked material.

4. Herbig-Haro objects which have high proper motions, and which are aligned with the CO lobes, can be interpreted as dense clumps of matter that have been accelerated by the jets. The clumps could have formed by thermal instability or entrainment in the vicinity of the nozzles, or else could represent local condensations in the cloud which intercept the paths of the jets. (The latter possibility could apply to the Herbig-Haro objects HH 1 and HH 2, where a recent encounter with the jets could have caused the original clumps to fragment.) The overall success of the shock emission model and the high degree of collinearity of the measured velocity vectors in objects like HH 1 and HH 2 provide strong support for this interpretation. An alternative interpretation in terms of Mach disks in an underexpanded, supersonic jet could perhaps apply to aligned Herbig-Haro objects which do not have detectable proper motions (but which may have large measured radial velocities). Herbig-Haro objects could be the counterparts of the emission knots that are often observed in extragalactic jets.

5. The broad-wing CO line emission arises in the shocked ambient material that is swept up by the expanding bubble or by the advancing jets. A similar emission pattern is expected in other molecules, and may be detected also in radiation from the shocked wind or jet. The separating CO lobes are the molecular-cloud analogs of extended extragalactic double radio sources. One advantage of interpreting the motion of CO lobes, as well as of Herbig-Haro objects, in terms of oppositely directed, supersonic jets is the substantial reduction (as compared with spherical-outflow models) in the inferred energy and momentum discharges at the source.

6. Bipolar nebulae could similarly be interpreted in terms of outflow into an anisotropic medium. The contours of the nebulae may correspond to the boundaries of interstellar bubbles which have elongated in the direction of the external density or pressure gradients. Alternatively, they may represent the boundaries of confined supersonic jets which are perturbed by variations in the external pressure distribution. Fan-shaped cometary nebulae could have formed after a bubble or jets broke out on one side of a dense cloud, but not on the other, or they could be bipolar nebulae viewed at sufficiently small angles to their axes, so that the counternebula is obscured from our view by the cloud.

7. The anistropy in the ambient medium could be induced either by rotation or by an ordered magnetic field. The latter possibility is indicated in at least some of the bipolar sources by polarization measurements. An ambient magnetic field could influence the expansion of an interstellar bubble both indirectly, through its effect on the external density distribution, and directly, by the action of magnetic stresses on the boundary, which becomes important after the velocity of the boundary drops to the value of the local (normal) Alfvén speed. An ordered magnetic field could give rise to an apparent bipolar molecular emission pattern even when the bubble remains spherical, provided that the central object is a strong source of dissociating UV photons.

In discussing the jet model for bipolar sources, we considered the source IRS 5 as a prototype, even though it is one of the least energetic in its class. This is because its relative proximity ($\sim$160 pc), and the large angle of the outflow direction with respect to the line of sight ($\sim$75°, based on the inferred velocity vector of HH 29), have enabled a detailed study of the CO lobes (Snell, Loren, and Plambeck 1980), a measurement of the proper velocities of the associated Herbig-Haro objects (Cudworth and Herbig 1979), as well as a radio and optical identification of the central "jet" (Cohen, Bieging, and Schwartz 1982; Strom, Grasdalen, and Strom 1974). Such favorable conditions are not always present in other bipolar sources. For example, the small angular separation of the blueshifted and the redshifted CO lobes in GL 490 (Lada and Harvey 1981) indicates that this source is observed at a small angle to the separation direction. Similarly, in the case of R Mon, the flattened molecular cloud surrounding the infrared object obscures the far side of the evacuated cavity from our view, and it is only through CO observations (Cantó *et al.* 1981) that the bipolar nature of the associated fan-shaped cometary nebula is revealed. It is, therefore, possible that certain features, which are predicted on this model and which are actually observed in some of the sources, may be difficult to detect in other bipolar sources because of a less favorable location or orientation. We also note that not all of the elements which have been included in the model would necessarily be present in each individual source. For example, in the case of the Herbig-Haro objects HH 1 and HH 2, the model predicts that two oppositely directed jets emanate from the central star. However, it is conceivable that there would be no CO lobes associated with these objects; this could occur, for instance, if the shock waves at the heads of the jets moved sufficiently fast ($V_h \gg 30$ km s^{-1}) to dissociate the swept-up CO molecules, and if the column density of the shocked material were still too low for these molecules to have re-formed (see McKee and Hollenbach 1980; Draine, Roberge and Dalgarno 1982). Nevertheless, extensive photometric, spectroscopic, and polarimetric studies of additional bipolar sources, carried out in various frequency bands, should be able to verify whether "jets," Herbig-Haro objects, separating CO lobes, and bipolar nebulae are indeed related through a basic outflow mechanism that is manifested on different scales. Such studies could also clarify some aspects of the model which are as yet not fully determined. Among the questions that remain to be answered are the exact role played by the ambient magnetic field in setting up the bipolar expansion and emission patterns in these sources, the relevance of certain wave phenomena that may occur in supersonic jets to the interpretation of bipolar nebulae and some Herbig-Haro objects, and the precise nature, parameters, and dynamical evolution of the putative stellar wind.

If the existence of supersonic jets near young stellar objects is indeed confirmed, then this would provide an additional proof that the jet phenomenon is widespread in astrophysics. Jets have first been identified and studied in active galactic nuclei, but they have now been observed also in the galactic source SS 443 (see Margon 1981 for a review), and their presence has been inferred in additional galactic objects, such as Sco X-1 (Hjellming and Wade 1971). It is conceivable that similar mechanisms are associated with the formation and propagation of jets on all of these scales. If this is the case, then molecular-cloud jets could serve as a unique probe of this phenomenon, due to their relative proximity and to the variety of observational techniques with which they can be studied. To illustrate this point, we note that if molecular emission lobes are indeed associated with "working surfaces" at the heads of jets, then this is the first instance of jets in which the motion of the heads has actually been measured. The velocity of the heads, together with the inferred ambient density in the cloud, could be used to place important constraints on the parameters of the jets (see eq. [12]). The study of jets in molecular clouds could also provide new insights into the environmental factors which determine the evolution of jets. In particular, the dynamical influence of the ambient magnetic field, which we considered on the basis of the apparent correlation between the direction of the field and the orientation of the bipolar axis, could perhaps be important also in other astrophysical environments. For example, it is conceivable that magnetic fields play a role in determining the density and pressure distributions of the gas "cloud" near the core of an active galactic nucleus, much as they are believed to do near the collapsed core of a dense molecular cloud. Another effect, the confinement of nozzles by ram pressure, was suggested in § III*b* as a possible solution to the apparent difficulty of maintaining static pressure support on simple models of protostellar environments. The same difficulty is encountered in the modeling of jets in active galactic nuclei (Smith *et al.* 1981). For jets in molecular clouds, this question could perhaps be elucidated by further high-resolution studies of the density and temperature distributions in the cores of the clouds.

During the course of this work, I have benefited from discussions with many colleagues on the various aspects of bipolar sources. I acknowledge, in particular, valuable suggestions from J. Arons, R. Blandford, and C. McKee, as well as useful conversations with J. Bieging, L. Blitz,

M. Cohen, J. Giuliani, G. Herbig, P. Ho., D. Hollenbach, R. Klein, T. Mouschovias, R. Plambeck, F. Shu, J. Silk, and C. Wetherill. I also thank the Aspen Center for Physics, where part of this work was performed, for hospitality. This research was supported by NSF grant AST 79-23243.

APPENDIX

EXPANSION OF AN ENERGY-DRIVEN INTERSTELLAR BUBBLE IN AN ANISOTROPIC MEDIUM

a) Anistropic Density Distribution

We consider the evolution of an energy-driven interstellar bubble which expands in an anisotropic density distribution. The bubble will elongate in the direction of the steepest density gradient, which we take to be along the z axis. Examination of equations (1), (2), (4), and (5) in the text, which describe the expansion when the medium is isotropic, reveals the main difficulties which are encountered in the solution for the anisotropic case. First, since the shape of the bubble is not known *a priori*, one cannot write down in advance the explicit dependence of the surface area or the volume on the coordinates. Second, for a similar reason, and also because not all the ambient material accumulates at the point where it is first intercepted, the mass of a given shell element cannot be specified in a simple manner. With regard to the second difficulty, we note the following properties of the solution (eq. [6] in the text) for a spherically symmetric bubble which expands in a medium with a density distribution $\rho_e(R) = \rho_0(R/R_0)^{-m}$; at any instant t, the solution satisfies

$$V_s^2(t) = \alpha(m)\frac{p(t)}{\rho_e[R_s(t)]}; \qquad p(t) = \frac{(2/3)E(t)}{\mathrm{Vol}(t)}; \qquad E(t) = \beta(m)L_w t\,, \tag{A1}$$

where $\alpha(m) = [1 + (m-2)/3(3-m)]^{-1}$, $\beta(m) = (5-m)/(3-m)$, and $\mathrm{Vol}(t)$ is the volume of the bubble. The relevant observation is that $\alpha(m)$ and $\beta(m)$ are slowly varying functions of m for m in the range 0 to 2 appropriate to a nonaccelerating bubble [$\alpha(m)\beta(m)$ changes only from 0.58 to 0.33 in this range]. This suggests that, even for an anisotropic expansion, the equation of motion could be approximated by $V_s^2 = \alpha p/\rho_e$, in which case the explicit dependence on the mass would be eliminated. This simplification implies, however, that the effects of mass flow within the shell (e.g., Giuliani 1982) also have to be neglected. The first difficulty can be tackled in the case of a one-dimensional density distribution by a suitable change of variables. This approach is based on the Kompaneets (1960) approximation to a point explosion in an exponential atmosphere (see also Dyson 1977). We confine our attention to a density distribution of the form $\rho_e(z) = \rho_0(z/z_0)^{-m}$, and describe the boundary of the bubble in cylindrical coordinates by the function $r(z, t)$. The volume is then given by

$$\mathrm{Vol}(t) = 2\pi\int_0^{z_{\max}(t)} r^2(z', t)dz'\,,$$

with $z_{\max}$ satisfying $r(z_{\max}) = 0$, and the velocity of the shell is $V_s(z, t) = (\partial r/\partial t)[1 + (\partial r/\partial z)^2]^{-1}$. On the basis of our previous discussion, we approximate the equation of motion by $V_s^2 = \frac{2}{3}\alpha(m)\beta(m)L_w t/\rho_e \mathrm{Vol}(t)$. With the help of the auxiliary variable

$$y = \left[\frac{2}{3}\frac{\alpha(m)\beta(m)L_w}{\rho_0}\right]^{1/2}\int_0^t \frac{t'^{1/2}dt'}{[\mathrm{Vol}(t')]^{1/2}}\,,$$

this becomes

$$\left(\frac{\partial r}{\partial y}\right)^2 - \left(\frac{z}{z_0}\right)^m\left[1 + \left(\frac{\partial r}{\partial z}\right)^2\right] = 0\,. \tag{A2}$$

As in the Kompaneets solution, we assume that, as long as the departure from sphericity is not too large, the solution satisfies

$$r = \xi y + \int_0^z [\xi^2(z'/z_0)^{-m} - 1]^{1/2}dz'; \qquad \frac{\partial r}{\partial \xi} = 0\,, \tag{A3}$$

where ξ is a separation variable. Equation (A3) can be solved in closed form for $m = 0$, 1, and 2. For $m = 0$, we recover the original spherically symmetric solution. In this case y can be identified as the radius R_s of the shell, and $\xi = R_s/r$. For $m = 1$, the solution is

$$r = z^{1/2}(\xi^2 z_0 - z)^{1/2} + \tfrac{1}{2}\xi y\,; \qquad z = \xi^2 z_0 \sin^2 (y/2\xi z_0)\,. \tag{A4}$$

This solution is plotted in Figure 1*a*. In this case $z_{max} = y^2/4z_0$, and the boundary intercepts the equatorial plane at $r = z_{max}/\pi$. The maximum value of r is $r_{max} = 2z_{max}/\pi$, which is attained at $z(r_{max}) = 4z_{max}/\pi^2$. The volume of the bubble scales as y^6, and hence, from the defining relation for y, $y \propto t^{3/8}$. The bubble therefore grows as $t^{3/4}$. For $m = 2$, the solution is

$$r^2 = z(V_{max}\, t - z)\,, \tag{A5}$$

where $V_{max} \approx [(2/3\pi)(L_w/\rho_0 z_0{}^2)]^{1/3}$ is the constant expansion speed of the bubble's ends. In this case the bubble is described by two osculating spheres, each of radius $z_{max}/2$, centered at $z = \pm z_{max}/2$ (Fig. 1*b*). Note that the solutions (A4) and (A5) each represent a self-similar expansion, and that, for this reason, the size of the bubble has the same dependence on time as in the spherically symmetric case ($R_s \propto t^{3/(5-m)}$; eq. [6]). This behavior, which is a consequence of our assumption that the source is located at the origin, characterizes all the solutions of equation (A3), including those which cannot be integrated in closed form, and applies also to the corresponding solutions for a momentum-driven bubble. The condition for an accelerated expansion ($m > 2$) is thus the same for strictly one-dimensional and for spherically symmetric density distributions. In the more general case when the density falls off also in the radial direction as some power l of r ($0 < l < m$), we again expect the shell to accelerate for $m > 2$. In this case the expansion is no longer self-similar, but the overall shape of the bubble at any given time should still resemble the curves in Figure 1.

b) Dynamical Interaction with an Ambient Magnetic Field

An interstellar bubble could elongate also as a result of interaction with an anisotropic external pressure distribution. An illustrative example is provided by a magnetic-pressure-dominated medium which contains a "frozen-in," uniform magnetic field B_0 directed along the z axis. If the density is also uniform, then an energy-driven bubble expanding in this medium would be roughly spherical as long as the internal pressure $p(t)$ is much larger than $p_e = 9B_0{}^2/32\pi$. (This is the magnetic pressure at the equator, which includes the effect of the stresses induced by the exclusion of the magnetic field from the cavity.) The anisotropy of the external pressure would cause the bubble to develop an ellipticity $e(t)$, which can be approximated by $e(t) = 1 - R_s'(t)/R_s(t)$, where $R_s(t)$ is given by equation (6) with $m = 0$, and $R_s'(t)$ is obtained by solving equations (1), (2), (4), and (5) in the text, and substituting $(p - p_e)$ for p on the right-hand side of equation (1) (cf. Heiligman 1980). In the limit $p_e/p(t) \ll 1$, these equations can be solved by a series expansion, with the result

$$e(t) = \frac{35}{347}\frac{p_e}{p(t)} = 0.08\left(\frac{B_0}{10^{-4}\ \mathrm{G}}\right)^2\left(\frac{L_w}{L_\odot}\right)^{-2/5}\left(\frac{\rho_e}{10^{-21}\ \mathrm{g\ cm^{-3}}}\right)^{-3/5}\left(\frac{t}{10^4\ \mathrm{yr}}\right)^{4/5}. \tag{A6}$$

We next consider the evolution of the bubble after the internal pressure has dropped to the value of the external (equatorial) pressure. The main body of the bubble (excluding the ends, whose exact shape is not important for our estimates) can then be approximated by a cylinder of radius R and length $2Z$. The ends of the bubble are not directly affected by the magnetic field, and consist of dense layers of shocked, swept-up ambient material. On the sides, however, the outer shock has disappeared, and the bubble is separated from the external magnetized medium by a contact discontinuity, across which the pressure is continuous. The pressure-balance condition can be approximated by

$$p = \left(1 + \frac{R^2}{Z^2}\right)\frac{B_0{}^2}{8\pi}\,, \tag{A7}$$

where the second term in parentheses represents the magnetic stresses induced by the exclusion of the field from the interior of the bubble (cf. Levy 1971). The evolution of the bubble then follows from equations (1), (2), (4), (5), (A7), and the given external density distribution, which we take to be of the form $\rho_e(z) = Az^{-m}$ ($0 \le m < 2$). As a zeroth-order approximation, we assume that $R^2/Z^2 \ll 1$, and neglect the second term on the right-hand side of equation (A7). We then find that

$$Z_0(t) \propto t^{2/(2-m)}\,; \qquad R_0(t) \propto t^{-m/(4-2m)}\,, \tag{A8}$$

so that $R_0{}^2/Z_0{}^2 \propto t^{-(4+m)/(2-m)}$ eventually becomes much less than unity, as required for self-consistency. The first-order corrections to Z_0 and R_0, Z_1 and R_1, can be obtained by including the second term in equation (A7) as a perturbation to the zeroth-order solution; this gives $Z_1/Z_0 = R_1/R_0 = R_0{}^2/Z_0{}^2$. Equation (A8) indicates that, for $m = 0$, the bubble elongates at a uniform rate and maintains a constant radius, while for $m > 0$ the ends of the bubble accelerate, and the

side walls move in. The decrease in R for $m > 0$ should probably be interpreted as a "pinching" motion in the equatorial region (see Poukey 1969; Levy 1971). As soon as the ends of the bubble start accelerating, they too may pinch as a result of the Rayleigh-Taylor instability. This, in turn, could lead to the formation of de Laval nozzles, as discussed in § III*a*.

REFERENCES

Barral, J. F., and Cantó, J. 1981, *Rev. Mexicana Astr. Ap.*, **5**, 101.
Beckwith, S., Persson, S. E., Neugebauer, G., and Becklin, E. E. 1978, *Ap. J.*, **223**, 464.
Begelman, M. C., Blandford, R. D., and Rees, M. J. 1982, *Rev. Mod. Phys.*, in preparation.
Beichman, C., and Harris, S. 1979, *Bull. AAS*, **11**, 713.
Benford, G. 1981, *Ap. J.*, **247**, 792.
Blandford, R. D., and Königl, A. 1979*a*, *Ap. Letters*, **20**, 15.
———. 1979*b*, *Ap. J.*, **232**, 34.
Blandford, R. D., and Rees, M. J. 1974, *M.N.R.A.S.*, **169**, 395.
Blitz, L., and Thaddeus, P. 1980, *Ap. J.*, **241**, 676.
Bodenheimer, P., Tenorio-Tagle, G., and Yorke, H. W. 1979, *Ap. J.*, **233**, 85.
Böhm, K. H., Böhm-Vitense, E., and Brugel, E. W. 1981, *Ap. J.* (*Letters*), **245**, L113.
Burton, W. B. 1976, *Ann. Rev. Astr. Ap.*, **14**, 275.
Calvet, N., and Cohen, M. 1978, *M.N.R.A.S.*, **182**, 687.
Cantó, J. 1980, *Astr. Ap.*, **86**, 327.
Cantó, J., and Rodríguez, L. F. 1980, *Ap. J.*, **239**, 982.
Cantó, J., Rodríguez, L. F., Barral, J. F., and Carral, P. 1981, *Ap. J.*, **244**, 102.
Castor, J., McCray, R., and Weaver, R. 1975, *Ap. J.* (*Letters*), **200**, L107.
Chan, K. L., and Henriksen, R. N. 1980, *Ap. J.*, **241**, 534.
Chernoff, D. F., Hollenbach, D. J., and McKee, C. F. 1982, *Ap. J.* (*Letters*), **259**, L97.
Cohen, M. 1973, *Ap. J.* (*Letters*), **185**, L75.
———. 1974, *Pub. A.S.P.*, **86**, 813.
———. 1982, *Pub. A.S.P.*, **94**, 266.
Cohen, M., Bieging, J. H., and Schwartz, P. R. 1982, *Ap. J.*, **253**, 707.
Cohen, M., Kuhi, L. V., Harlan, E. A., and Spinrad, H. 1981, *Ap. J.*, **245**, 920.
Cohen, M., and Schwartz, R. D. 1979, *Ap. J.* (*Letters*), **233**, L77.
Courant, R., and Friedrichs, K. O. 1948, *Supersonic Flow and Shock Waves* (New York: Interscience), chaps. IV and V.
Craine, E. R., Boeshaar, G. O., and Byard, P. L. 1981, *A.J.*, **86**, 751.
Cudworth, K. M., and Herbig, G. 1979, *A.J.*, **84**, 548.
DeCampli, W. M. 1981, *Ap. J.*, **244**, 124.
De Young, D. S., and Axford, W. I. 1967, *Nature*, **216**, 129.
Downes, D., Genzel, R., Becklin, E. E., and Wynn-Williams, C. G. 1981, *Ap. J.*, **244**, 869.
Downes, D., Genzel, R., Hjalmarson, Å., Nyman, L. Å., and Rönnäng, B. 1982, *Ap. J.* (*Letters*), **252**, L29.
Draine, B. T. 1979, *Ap. Space Sci.*, **65**, 313.
Draine, B. T., and Roberge, W. G. 1982, *Ap. J.* (*Letters*), **259**, L91.
Draine, B. T., Roberge, W. G., and Dalgarno, A. 1982, *Ap. J.*, in press.
Dyck, H. M., and Lonsdale, C. J. 1979, *A.J.*, **84**, 1339.
Dyson, J. E. 1977, *Astr. Ap.*, **59**, 161.
Elias, J. H. 1980, *Ap. J.*, **241**, 728.
Elmegreen, B. G. 1978, *Moon and Planets*, **19**, 261.
Field, G. B., Rather, J. D. G., Annestad, P. A., and Orszag, S. A. 1968, *Ap. J.*, **151**, 953.
Fridlund, C. V. M., Nordh, H. L., van Duinen, R. J., Aalders, J. W. G., and Sargent, A. I. 1980, *Astr. Ap.*, **91**, L1.
Garrison, L. M., Jr. 1978, *Ap. J.*, **224**, 535.
Genzel, R., Reid, M. J., Moran, J. M., and Downes, D. 1981, *Ap. J.*, **244**, 884.
Giuliani, J. L., Jr. 1982, *Ap. J.*, **256**, 624.
Glassgold, A. E., and Langer, W. D. 1975, *Ap. J.*, **197**, 347.
Goldreich, P., and Kylafis, N. D. 1981, *Ap. J.* (*Letters*), **243**, L75.
Gull, S. F., and Northover, K. J. E. 1973, *Nature*, **244**, 80.
Hardee, P. E. 1979, *Ap. J.*, **234**, 47.
Harvey, P. M., Campbell, M. F., and Hoffmann, W. F. 1977, *Ap. J.*, **215**, 151.
Heiligman, G. M. 1980, *M.N.R.A.S.*, **191**, 761.
Herbig, G. H., and Jones, B. F. 1981, *A.J.*, **86**, 1232.
Hill, J. K., and Hollenbach, D. J. 1978, *Ap. J.*, **225**, 390.
Hjellming, R. M., and Wade, C. M. 1971, *Ap. J.* (*Letters*), **164**, L1.
Hollenbach, D., Chu, S. I., and McCray, R. 1976, *Ap. J.*, **208**, 458.
Hollenbach, D., and McKee, C. F. 1979, *Ap. J. Suppl.*, **41**, 555.
Icke, V. 1981, *Ap. J.*, **247**, 152.
Kompaneets, A. 1960, *Soviet Phys. Doklady*, **5**, 46.
Kuhi, L. V. 1964, *Ap. J.*, **140**, 1409.
Kulsrud, R. M., Berstein, I. B., Kruskal, M., Fanucci, J., and Ness, N. 1965, *Ap. J.*, **142**, 491.
Lada, C. J., and Harvey, P. M. 1981, *Ap. J.*, **245**, 58.
Larson, R. B. 1981, *M.N.R.A.S.*, **194**, 809.
Levy, E. H. 1971, *Ap. J.*, **164**, 23.
Lonsdale, C. J., Dyck, H. M., Capps, R. W., and Wolstencroft, R. D. 1980, *Ap. J.* (*Letters*), **238**, L31.
Margon, B. 1981, *Ann. NY Acad. Sci.*, **375**, 403.
Martin, P. G. 1974, *Ap. J.*, **187**, 461.
Mathews, W. G. 1966, *Ap. J.*, **143**, 173.
McKee, C. F., and Cowie, L. L. 1975, *Ap. J.*, **195**, 715.
McKee, C. F., Cowie, L. L., and Ostriker, J. P. 1978, *Ap. J.* (*Letters*), **219**, L23.
McKee, C. F., and Hollenbach, D. J. 1980, *Ann. Rev. Astr. Ap.*, **18**, 219.
Melnick, G., and Harwit, M. 1975, *M.N.R.A.S.*, **171**, 441.
Mouschovias, T. Ch. 1976, *Ap. J.*, **207**, 141.
———. 1978, in *Protostars and Planets*, ed. T. Gehrels (Tucson: University of Arizona Press), p. 209.
Nadeau, D., and Geballe, T. R. 1979, *Ap. J.* (*Letters*), **230**, L169.
Norman, C. A., and Silk, J. 1979, *Ap. J.*, **228**, 197.
Norman, M. L., Smarr, L., Wilson, J. R., and Smith, M. D. 1981*a*, *Ap. J.*, **247**, 52.
Norman, M. L., Smarr, L., Winkler, K-H. A., and Smith, M. D. 1981*b*, preprint.
Pai, S-I. 1953, *Fluid Dynamics of Jets* (New York: Van Nostrand), chap. III.
Phillips, J. P., and Beckman, J. E. 1980, *M.N.R.A.S.*, **193**, 245.
Pikel'ner, S. B. 1968, *Ap. Letters*, **2**, 97.
Plambeck, R. L., Wright, M. C. H., Welch, W. J., Bieging, J. H., Baud, B., Ho, P. T. P., and Vogel, S. N. 1982, *Ap. J.*, **259**, 617.
Poukey, J. W. 1969, *Phys. Fluids*, **12**, 1452.
Rees, M. J. 1978, *M.N.R.A.S.*, **184**, 61.
Rodríguez, L. F., Ho, P. T. P., and Moran, J. M. 1980, *Ap. J.* (*Letters*), **240**, L149.
Scheuer, P. A. G. 1974, *M.N.R.A.S.*, **166**, 513.
Schmidt, G. D., and Cohen, M. 1981, *Ap. J.*, **246**, 444.
Schwartz, R. D. 1978, *Ap. J.*, **223**, 884.
———. 1981, *Ap. J.*, **243**, 197.
Shu, F. H. 1977, *Ap. J.*, **214**, 488.
Shull, J. M. 1980, *Ap. J.*, **238**, 860.
Shull, J. M., and McKee, C. F. 1979, *Ap. J.*, **227**, 131.
Simon, M., Felli, M., Cassar, L., Fischer, J., and Massi, M. 1982, preprint.
Simon, M., Righini-Cohen, G., Fischer, J., and Cassar, L. 1981, *Ap. J.*, **251**, 552.
Smith, M. D., Smarr, L., Norman, M. L., and Wilson, J. R. 1981, preprint.
Snell, R. L. 1979, Ph.D. thesis, University of Texas at Austin.
Snell, R. L., and Edwards, S. 1981, *Ap. J.*, **251**, 103.
———. 1982, *Ap. J.*, **259**, 668.
Snell, R. L., Loren, R. B., and Plambeck, R. L. 1980, *Ap. J.* (*Letters*), **239**, L17.
Sparke, L. S. 1982, *Ap. J.*, **260**, 104.
Spitzer, L., Jr. 1978, *Physical Processes in the Interstellar Medium* (New York: Wiley-Interscience), chap. 8.
Stahler, S. W., Shu, F. H., and Taam, R. E. 1980, *Ap. J.*, **241**, 637.

Steigman, G., Strittmatter, P. A., and Williams, R. E. 1975, *Ap. J.*, **198**, 575.
Strom, S. E., Grasdalen, G. L., and Strom, K. M. 1974, *Ap. J.*, **191**, 111.
Thompson, R. I., and Tokunaga, A. T. 1979, *Ap. J.*, **231**, 736.
Torrelles, J. M., Rodríguez, L. F., Cantó, J., Moran, J. M., Ho, P. T. P., and Marcaide, J. 1981, *Bull. AAS*, **13**, 854.
Vrba, F. J., Coyne, G. V., and Tapia, S. 1981, *Ap. J.*, **243**, 489.
Vrba, F. J., Strom, S. E., and Strom, K. M. 1976, *A.J.*, **81**, 958.
Weaver, R., McCray, R., Castor, J., Shapiro, P., and Moore, R. 1977, *Ap. J.*, **218**, 377.
Wiita, P. J. 1978, *Ap. J.*, **221**, 436.
Wouterloot, J. G. A., Habing, H. J., and Herman, J. 1980, *Astr. Ap.*, **81**, L11.
Wright, A. E., and Barlow, M. J. 1975, *M.N.R.A.S.*, **170**, 41.
Zel'dovich, Ya.B., and Raizer, Yu.P. 1967, *Physics of Shock Waves and High-Temperature Hydrodynamic Phenomena* (New York: Academic Press), chap. XII.

ARIEH KÖNIGL: Astronomy Department, University of California, Berkeley, CA 94720